Bioorganic & Medicinal Chemistry Vol. 1, No. 4, pp. 285-307, 1993
Printed in Great Britain

0968-0896/93 $6.00 + .00

1-Benzazepin-2-one Calcium Channel Blockers—VI. Receptor-binding Model and Possible Relationship to Desmethoxyverapamil.

S. David Kimball,*[a] John T. Hunt,[a] Joel C. Barrish,[a] Jagabandhu Das,[a] David M. Floyd,[a] Michael W. Lago,[a] Ving G. Lee,[a] Steven H. Spergel,[a] Suzanne Moreland,[b] S. Anders Hedberg,[b] Jack Z. Gougoutas,*[c] Mary F. Malley[c] and Wan F. Lau[d]

[a]*Cardiovascular Chemistry,* [b]*Pharmacology,* [c]*Solid State Chemistry,* [d]*Computer-Assisted Drug Design/Chemistry-Core Resources, Bristol-Myers Squibb Pharmaceutical Research Institute, P.O. Box 4000, Princeton, NJ 08543-4000*

(*Received* 14 *June* 1993; *accepted* 23 *July* 1993)

Abstract—We have prepared a series of potent antihypertensive 1-benzazepin-2-one calcium channel blockers (CCBs) **1** that are structurally related to diltiazem **2**. Structural studies and the preparation of conformationally constrained analogs of 1-benzazepin-2-ones have led us to postulate a receptor-bound conformation for both **1** and **2**. We believe that these compounds bind to the calcium channel protein in an MI ("inboard") binding conformation in which the amine of the side chain is placed over the heptagonal benzazepinone ring and in close proximity to the phenyl methyl ether pharmacophore. This receptor-bound conformation places the side chain amine and methyl ether pharmacophores in the same spatial relationship as 3-methoxy phenylethylamine. Combined with our SAR, this binding model rationalizes literature findings that desmethoxyverapamil can demonstrate pharmacology typical of both phenylalkylamine (PA) and benzothiazepinone (DTZ) calcium channel blockers. Simple experiments are proposed to test the hypothesis that desmethoxyverapamil can bind at the benzothiazepinone site on the calcium channel.

Introduction

We have described the synthesis of 1-benzazepin-2-one calcium channel blockers (CCBs) **1** that are structurally related to diltiazem **2** (Figure 1).[1,2] The structure–activity relationships (SAR) of this new class of CCBs have been elaborated[2–4] and shown to parallel the SAR of benzothiazepinone CCBs such as diltiazem. We have demonstrated that these compounds compete for the diltiazem binding site on the voltage-dependent calcium channel and, as with diltiazem, the appropriate absolute and relative stereochemistry in the benzazepinone/benzothiazepinone ring is important to activity *in vitro*.[2] Benzazepinones **1** have the same absolute and relative stereochemical preferences at the receptor as diltiazem. Two pharmacophores are critical to the activity of benzazepinones *in vitro* and *in vivo*,[4,5] a basic amino group appended to the amide of the benzazepinone ring, and a pendant 4-methoxyphenyl group at the C-4 position. These general conclusions are summarized in Figure 2.

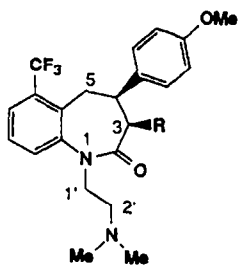

Benzazepinones **1**
a: R = Et
b: R = OAc

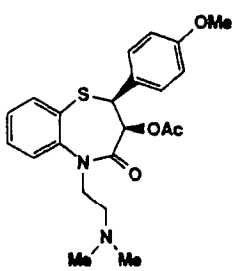

Diltiazem **2**

Figure 1.

The incorporation of drug metabolism data into the structure–activity relationships of the benzazepinones was critical to the discovery of CCBs of this class that are efficacious *in vivo*. The studies which allowed us to develop potent and long-acting benzazepinone antihypertensive agents have also been summarized previously.[2,5]

Consideration of the spatial relationship of the two pharmacophores in the solid state structures of many active and inactive derivatives suggested a fundamental conformational constraint: the heptagonal ring in receptor bound structures adopts an "M" twist-boat conformation in which the exocyclic N1–C1' (side chain) and C4–Ar bonds to the pharmacophores are directed toward the same side of the mean plane of the benzazepinone ring.[1] This conformational model requires further elaboration, however, since the spatial separation of the pharmacophores is further coupled to rotations about the two bonds of the side chain N1–C1'–C2', rotations which bring the basic nitrogen, N2, to either side of the plane of the lactam. We designate ω_1 and ω_2 as the torsional angles C2–N–C1'–C2' and N–C1'–C2'–N, respectively.

In this paper we describe the use of conformationally constrained side chains to explore the preferred spatial relationship between the two key pharmacophores of the benzazepinone and benzothiazepinone CCBs.[6,7] The resulting model describes the likely conformation of the compounds when bound to the calcium channel: the side chain is rotated "inboard" ($\omega_1 \sim 100°$) with N2 lying over the heptagonal ring and proximate to the methyl ether (ω_2

~ -60°). Interestingly, in this conformation the pharmacophores maintain approximately the same spatial relationship as those of fully extended 3-methoxy phenylethylamine. The SAR of the benzazepinones and their possible relationship to desmethoxyverapamil are rationalized in light of this model. This working hypothesis has also been used predictively, in the *de novo* design and synthesis of structurally distinct diltiazem-like CCBs (see following paper in this series).

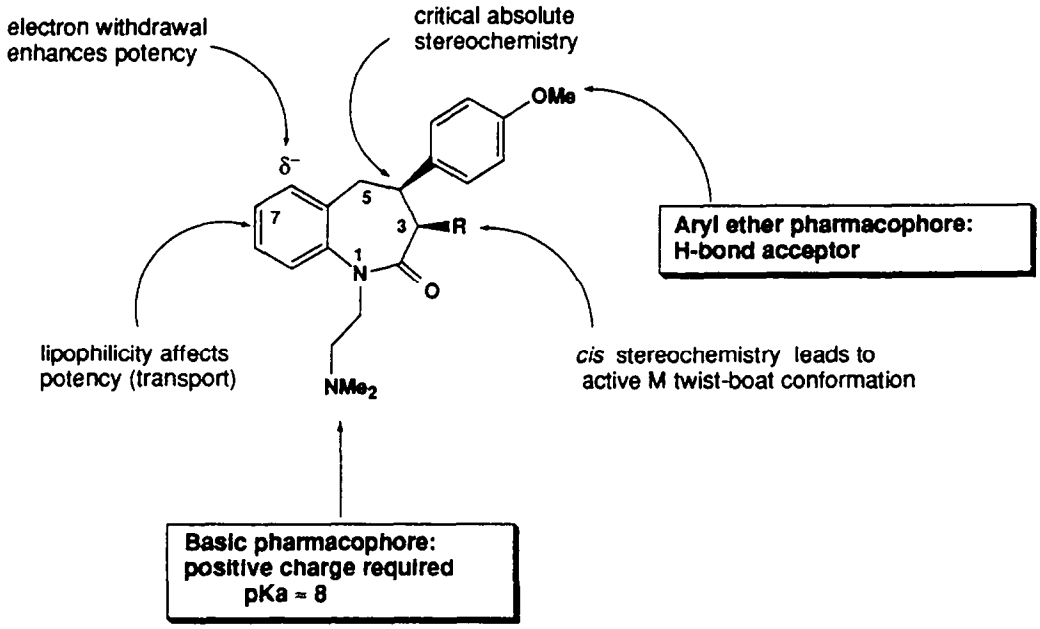

Figure 2. Key structural features and SAR of benzazepinone CCBs

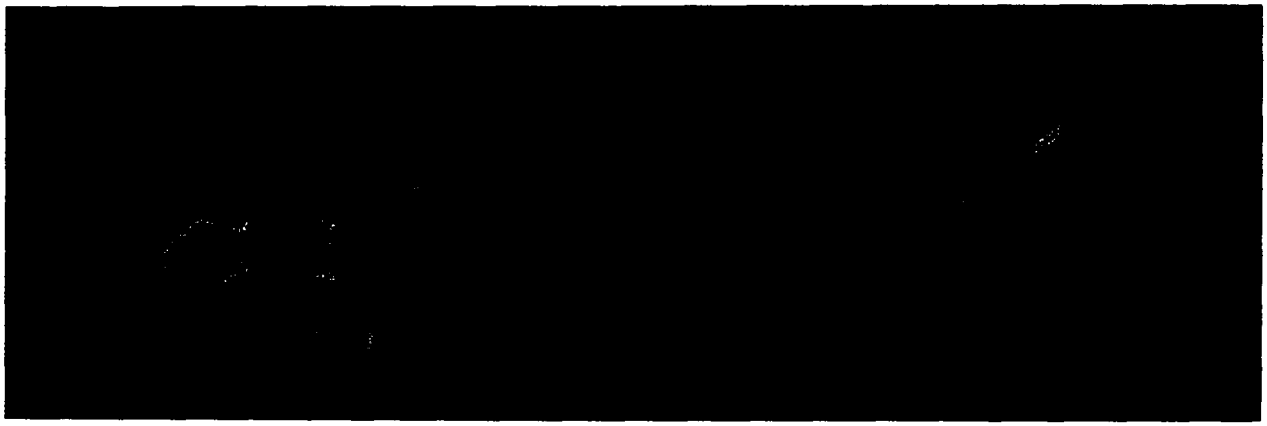

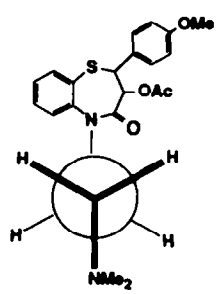

Diltiazem **2**
MO ("Outboard"): ω_1 = -80 °, ω_2 = 170°

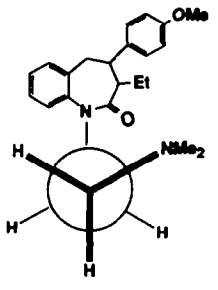

Benzazepinone **1a**
MI ("Inboard"): ω_1 = 101 °, ω_2 = -60°

Figure 3. Solid state conformation and Newman projections of benzazepinone **1a** and diltiazem **2**

Models of the Receptor-Bound Conformation

Examination of the conformational space of the amine pharmacophore shows that two distinct relationships between the benzazepinone pharmacophores are possible on binding to the calcium channel (Figure 3). Although the heptagonal ring has the same "M" twist boat conformation in both, the two conformations differ in having the pharmacophores on opposite sides (MO, "outboard") or the same side (MI, "inboard") of the plane of the lactam. This generally requires that the torsional angle $\omega_1 < 0°$ for MO conformations and $\omega_1 > 0°$ for MI conformations. The MO conformation is illustrated by the solid state structure of diltiazem **2**[8] ($\omega_1 = -80°$, $\omega_2 = 170°$). The MI conformation is illustrated by the solid state structure of benzazepinone **1a** ($\omega_1 = 101°$, $\omega_2 = -60°$).

Both MO and MI conformations of the benzazepinone side chain have been observed in crystal structures of several benzazepinone calcium channel blockers (Table 1). The NMR solution structure (CD_2Cl_2) of diltiazem[9] as well as benzazepinone **1b** (data not shown) is most consistent with an MO conformation in which the side chain is rotated "outboard" and extended ($\omega_2 \sim 180°$). However, calculations using molecular mechanics (MM2) show little difference between the energy of the MO or MI conformations for benzazepinones such as **1** (data not shown).

A priori, either binding mode MO or MI could be the conformation of the receptor-bound structure. We therefore decided to test these binding models by synthesizing conformationally constrained benzazepinone analogs.

Table 1.

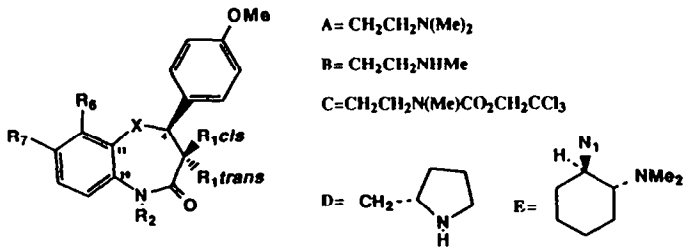

Compound	R_2	R_1 *cis*	R_1 *trans*	R_6	R_7	X	ϕ_R[c]	ϕ_e	ω_1	ω_2
1a	A	Et	H	CF_3	H	CH_2	-42	54	101	-61
2	A	OAc	H	H	H	S	-42	50	-80	170
3	A	Me	H	CF_3	H	CH_2	-46	53	82	170
4	D	OAc	H	CF_3	H	CH_2	-36	75	-83	87
8	E	Me	H	CF_3	H	CH_2	-47	56	-46,[f] -48	-49, -49
9	H	OH	H	CF_3	H	CH_2	-43	65		
SQ32,488[a]	H	H	OH	H	H	CH_2	+47	87		
SQ32,432[a]	H	H	CO_2Me	H	H	CH_2	+48	55		
SQ32,433[a]	H	Me	CO_2Me	H	H	CH_2	-40	52		
L203-161[a]	H	OH	H	H	H	CH_2	-46	64		
SQ31,098[b]	H	Me	H	H	Cl	CH_2	-41	63		
SQ32,324[b]	B	OAc	H	CF_3	H	CH_2	-51	41	109	-57
I895-069[b]	C	OAc	H	CF_3	H	CH_2	-41	59	81	-176
SQ32,651[b]	A	OH	H	CF_3	H	CH_2	-50	48	133	-56
SQ31,833[b]	H	H	CO_2^-	CF_3	H	CH_2	-36	76		
SQ32,064[c]	H	CO_2H	Et	CF_3	H	CH_2	-35	80		
SQ32,065[c]	H	Me	H	CF_3	H	CH_2	-46	53		
SQ31,828[c]	A	$CH_2CH=CH_2$	H	CF_3	H	CH_2	-44	47	104	-63
SQ32,256[c]	A	Bn	H	CF_3	H	CH_2	-46	56	97	-63
SQ31,992[c]	A	H	Et	CF_3	H	CH_2	+44	69	-74	-54
SQ34,172[d]	D	OAc	H	H	OMe	CH_2	-48	96	106	170
SQ34,172B[d]	D	OAc	H	H	OMe	CH_2	-48	38	113	170
SQ34,088[d]	D	OAc	H	H	OMe	S	-46	48	108	171

[a]Reference 1.
[b]Reference 2.
[c]Reference 3.
[d]Reference 5.
[e]Minus and plus values for this torsional angle Φ_R = X–C4–C3–C2, characterize the "M" and "P" twist boat conformations of the heptagonal ring. Φ_e is torsional angle X–C2–Car–Car, ω_1 is the C2–N–C1'–C2' torsional angle of the side chain, and ω_2 is the N–C1'–C2'–N torsional angle of the side chain.
[f]Two independent molecules in the asymmetric unit.

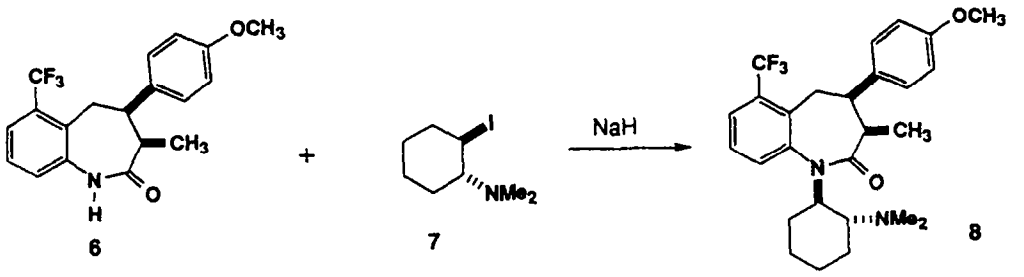

Scheme I. Synthesis of racemic 3-methyl benzazepinone **8**.

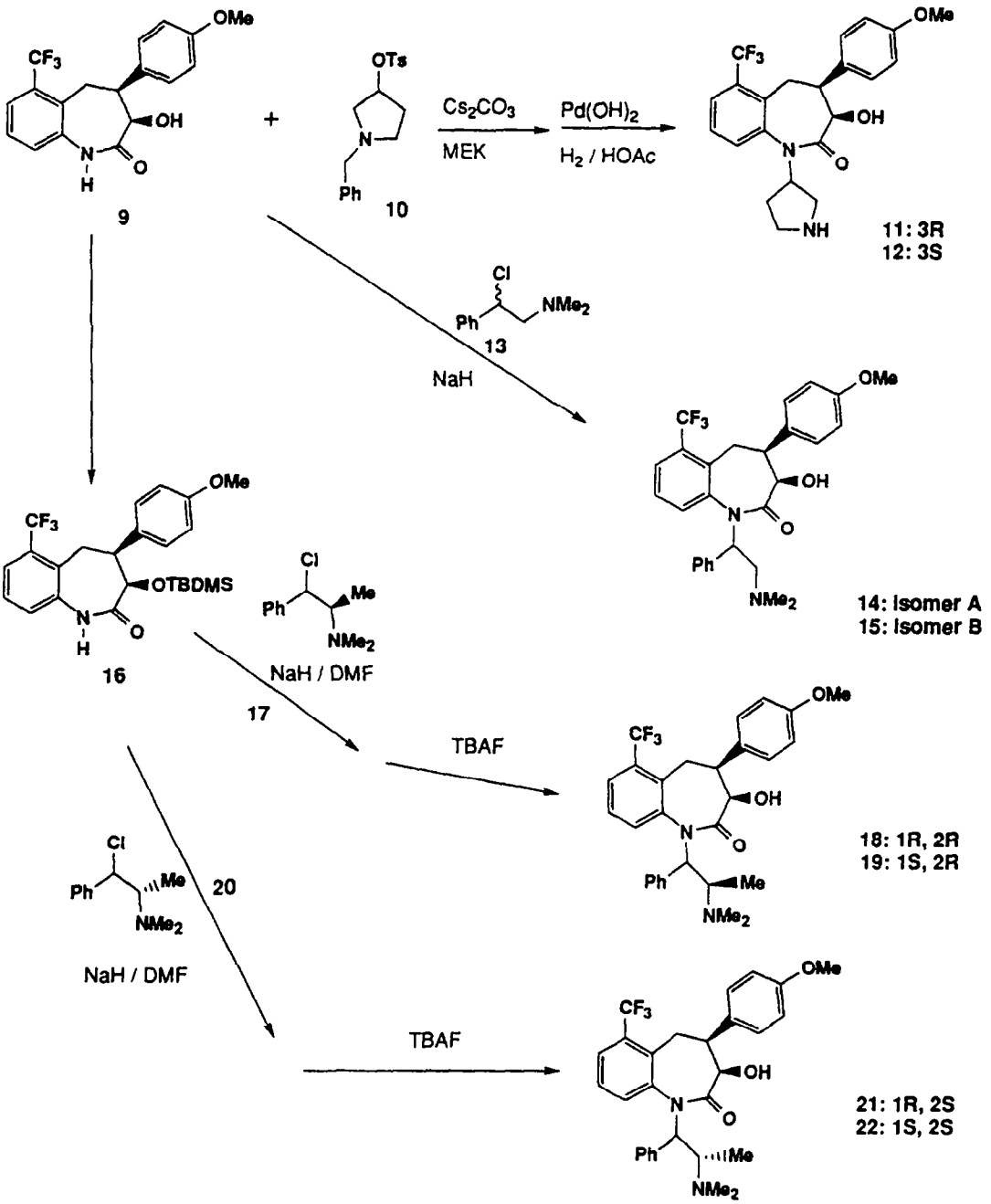

Scheme II. Synthesis of nonracemic 3-hydroxy benzazepinones.

Chemistry

The synthesis of compounds **3–5** has been described previously.[2–4] Compounds **23–25** were also prepared using the methodology detailed in previous papers.[2–4] Compound **8** was prepared by alkylation of 3-methyl benzazepinone **6** by *trans*-β-iodo-dimethylamino-cyclohexane[10] **7**, as shown in Scheme I. This reaction is believed to proceed via the aziridinium ion intermediate, to afford the *trans* isomer. The *trans* stereochemistry about the cyclohexyl ring was initially assigned by variable temperature ^{1}H NMR. At -30 °C, the methine hydrogens resolve into a ddd pattern with coupling constants of 4, 11, and 11 Hz, indicative of two *anti* periplanar couplings. We have also established the stereochemistry of compound **8** by X-ray crystallography (vide infra).

The synthesis of compounds **11–22** is depicted in Scheme II. Alkylation of the hydroxy benzazepinone **9** by tosylate **10**[11] or its enantiomer provided compounds **11** and **12**, respectively. These alkylation reactions proceeded smoothly using Cs_2CO_3 as the base, in MEK. Compounds **14** and **15** were prepared via alkylation of **9** by the free base of *N,N*-dimethyl-β-chloro-phenethylamine **13**.[12] Separation of the two diastereomeric products led to the α-phenyl analogs.

Compounds **18**, **19**, **21**, and **22** were prepared by alkylating the TBDMS ether **16** with the 3-phenyl-3-chloro-2-dimethylamino propanes **17** and **20**, as shown in Scheme II. The use of the TBDMS protecting group on **16** significantly increased the yield of these reactions with the hindered alkylating agents **17** and **20**, by reducing the amount of imidate formed. Compounds **17** and **20** were prepared from (1*S*, 2*R*) norephedrine and (1*R*, 2*S*) norephedrine, respectively. The assignment of stereochemistry for the derived chlorides was based on proton NMR. For compounds **17**, the 1*R*, 2*R* (predominant isomer, inversion of stereochemistry) had J = 7.6 Hz, while the 1*S*, 2*R* isomer had J = 0 Hz. For compounds **20**, the 1*R*, 2*S* isomer had J = 0 Hz, while the 1*S*, 2*S* isomer had J = 8.2 Hz. The alkylation of **16** by **17** and **20** is presumed to proceed via an aziridinium ion intermediate;[13] the absolute stereochemistry of the alkylating agent is thereby transferred to the product.

Physical data for new compounds **8**, **11**, **12**, **14**, **15**, **18**, **19**, **21**, and **22** are listed in Table 2.

Table 2. Physical data for new compounds

compd	R_1	R_2	Scheme	%yield[a]	mp	recryst solvent	formula	analysis[b]	optical rotation
8 (±)	Me	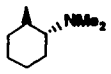	I	23%	>250°	iPA/Et_2O	$C_{27}H_{33}F_3N_2O_2$·HCl	CHNClF	-
11	OH		II	54%	214-215°	iPA	$C_{22}H_{23}F_3N_2O_3$·$C_4H_4O_4$	CHNClF	+58.9°(c=0.50,MeOH))
12	OH		II	51%	228-231°	MeOH/Et_2O	$C_{22}H_{23}F_3N_2O_3$·$C_4H_4O_4$	CHN	+57.8° (c=1.0, AcOH)
14	OH	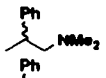	II	27%	136-142°	iPA/iPE	$C_{28}H_{29}F_3N_2O_3$·HCl	CHNClF	+146.2° (c=1.0, MeOH)
15	OH	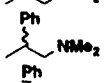	II	6%	165-171°	Et_2O	$C_{28}H_{29}F_3N_2O_3$·HCl	CHNClF	+221.8° (c=1.0, MeOH)
18 (1R,2R)	OH	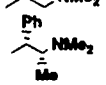	II	22%	>220°	Et_2O	$C_{29}H_{31}F_3N_2O_3$·HCl	CHNClF	+180.0° (c=1.0, MeOH)
19 (1S,2R)	OH	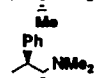	II	10%	191-192°	iPE/MeOH	$C_{29}H_{31}F_3N_2O_3$·HCl	CHNClF	+242.6° (c=1.05, MeOH)
21 (1R,2S)	OH	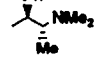	II	25%	148-151°	Et_2O	$C_{29}H_{31}F_3N_2O_3$·HCl	CHNClF	+167.6° (c=0.75, MeOH)
22 (1S,2S)	OH	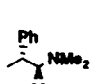	II	39%	233-235°	Et_2O	$C_{29}H_{31}F_3N_2O_3$·HCl	CHNClF	+174.7° (c=0.66, EtOH)

[a]Yield from intermediates **6**, **9**, or **16**.
[b]All compounds gave acceptable elemental analyses.

Tests of Hypothesis: Constrained Compounds

The compounds that test our binding hypotheses constrain the conformational space available to the basic amino group by substitution on the dimethylaminoethyl sidechain of compounds **1**. Substitution on the basic sidechain and, in particular, incorporating it into a ring limits the spatial orientation of the amino pharmacophore relative to the aryl methyl ether. Table 3 lists the set of constrained compounds prepared in this study, along with their activity *in vitro*.

Figures 4–6 illustrate the conformational space available to the basic amine pharmacophore for compound **3**. Figure 4 presents the solid state conformation of benzazepinone **3**, as determined in our laboratories ($\omega_1 = 82°$, $\omega_2 = 170°$). The blue surface of Figure 5 represents the locus of all possible positions of the amine resulting from rotations about the N–C1' (ω_1) and C1'–C2' (ω_2) carbon–carbon single bonds in the dimethylaminoethyl sidechain of **3**.

A crude conformational grid search of this locus for sterically accessible positions of the amine (within 10 Kcal/mol of the minimum estimate of non-bonded energy) was carried out; the blue spheres of Figure 6 represent the positions of the nitrogen atom for these "low" energy conformations. We have also carried out the same computation, but with MM2 minimization at each grid point; qualitatively, the results are the same. Conformations corresponding to both outboard (MO) and inboard (MI) binding modes are energetically accessible to **3**, as this compound has no structural constraints on the possible loci of the amine. In a previous publication, we identified compound **4** as a potent CCB *in vitro* and a long-acting antihypertensive agent.[2] Like the simple, unconstrained analog **3**, compounds **4** and **5** have minimal conformational constraints (data not shown). For both of these compounds, as for benzazepinone **3**, either the MO or MI families of conformations could be the receptor bound form.

Table 3. Activity of N1-substituted benzazepinones *in vitro* and *in vivo*

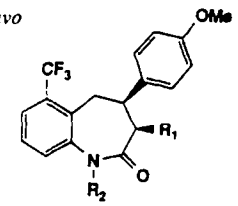

compd	R_1	R_2	log P (est'd)[a]	IC_{50}(μM)[b]	kd (μM)[c]
3 (±)	Me	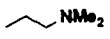	3.6	0.076 (0.041-0.14)	0.075 ± 0.043
4	OAc		2.1	0.091 (0.068-0.12)	0.13 ± 0.052
5	OAc		2.1	0.63 (0.38-1.0)	0.12 ± 0.011
8 (±)	Me	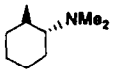	4.5	0.38 (0.22-0.67)	0.39[d]
11	OH		0.93	0.32 (0.19-0.55)	0.24 ± 0.14
12	OH		0.93	3.8 (2.2-6.4)	1.8 ± 0.38
14 (isomer A)	OH	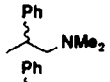	6.2	0.48 (0.34-0.68)	1.1[d]
15 (isomer B)	OH	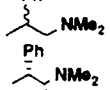	4.3	0.34 (0.24-0.50)	0.24[d]
18 (1R,2R)	OH	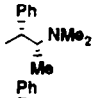	3.0	0.34 (0.23-0.52)	0.17[d]
19 (1S,2R)	OH	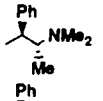	3.8	0.18 (0.12-0.26)	0.037[d]
21 (1R,2S)	OH	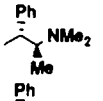		0.43 (0.27-0.67)	0.50 ± 0.23
22 (1S,2S)	OH	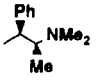	4.0	0.51 (0.24-1.1)	0.25 ± 0.018

[a]Log *P* estimated by reverse phase HPLC.[4]
[b]IC_{50} in rabbit aorta strips contracted with KCl (95% confidence interval).
[c]k_d Determined by displacement of radiolabeled diltiazem in guinea pig striated muscle (± SEM).
[d]Based on concentration–effect curve using one animal.

Figure 4. Solid state conformation of benzazepinone **3**

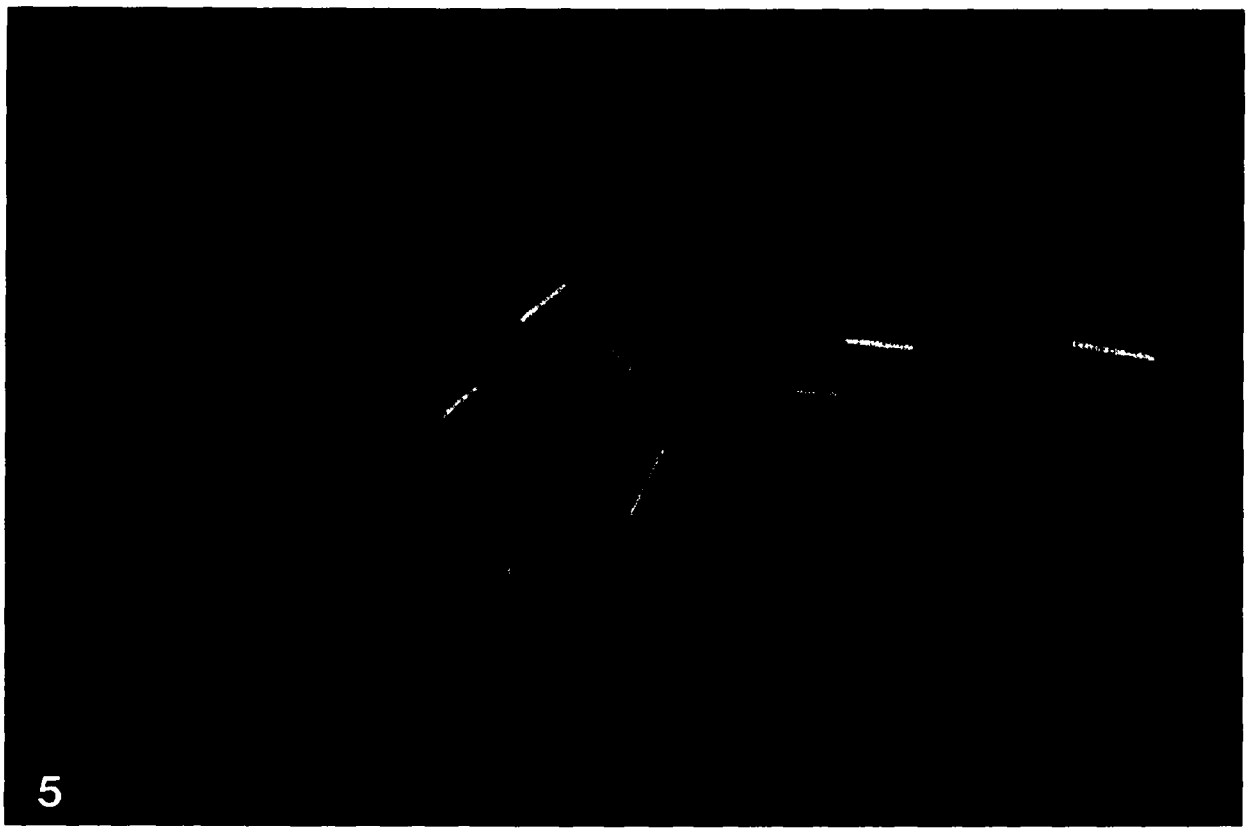

Figure 5. The surface of accessible positions of the amine in benzazepinone **3**, relative to a fixed heptagonal "M" twist-boat conformation

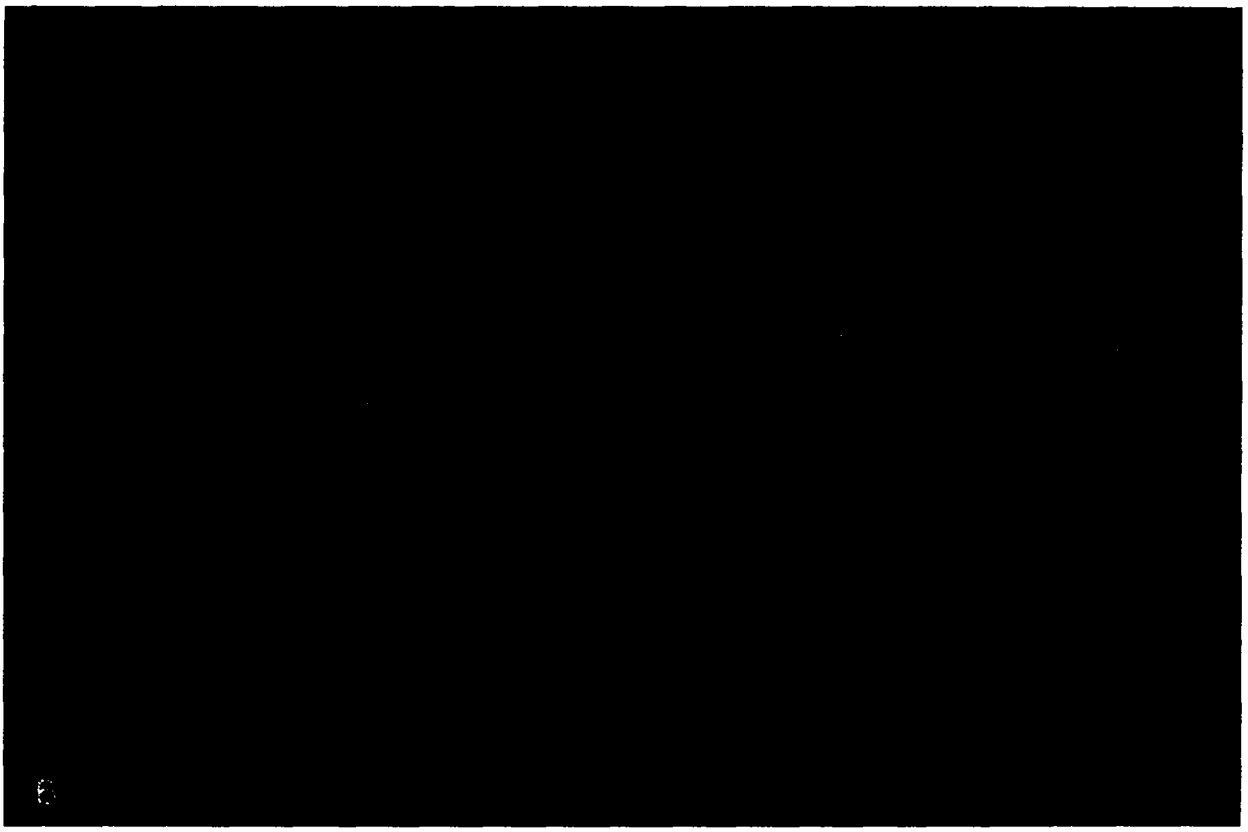

Figure 6. Energetically accessible conformations of the amine-benzazepinone **3**

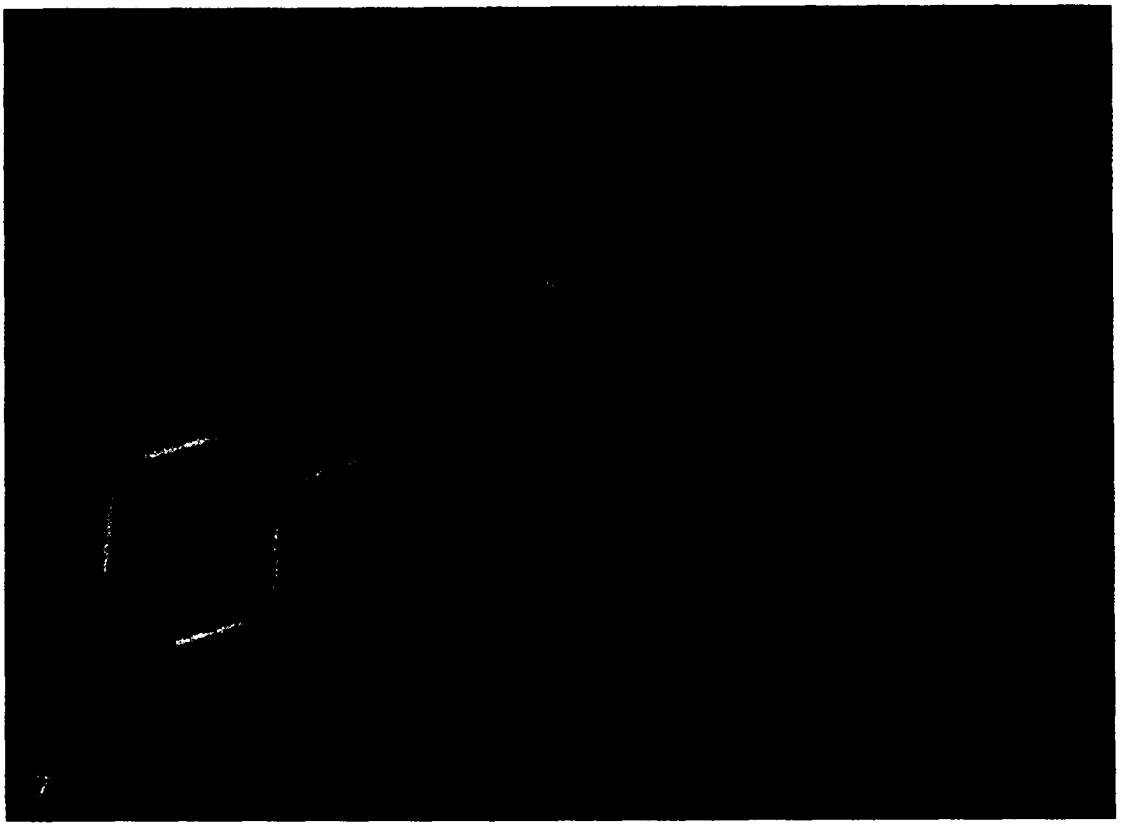

Figure 7. Solid state conformation of benzazepinone **8**

Figure 8. The accessible conformations of the amine in benzazepinone **8**, relative to a fixed heptagonal "M" twist-boat conformation

Figure 9. Energetically accessible conformations of the amine–benzazepinone **8**

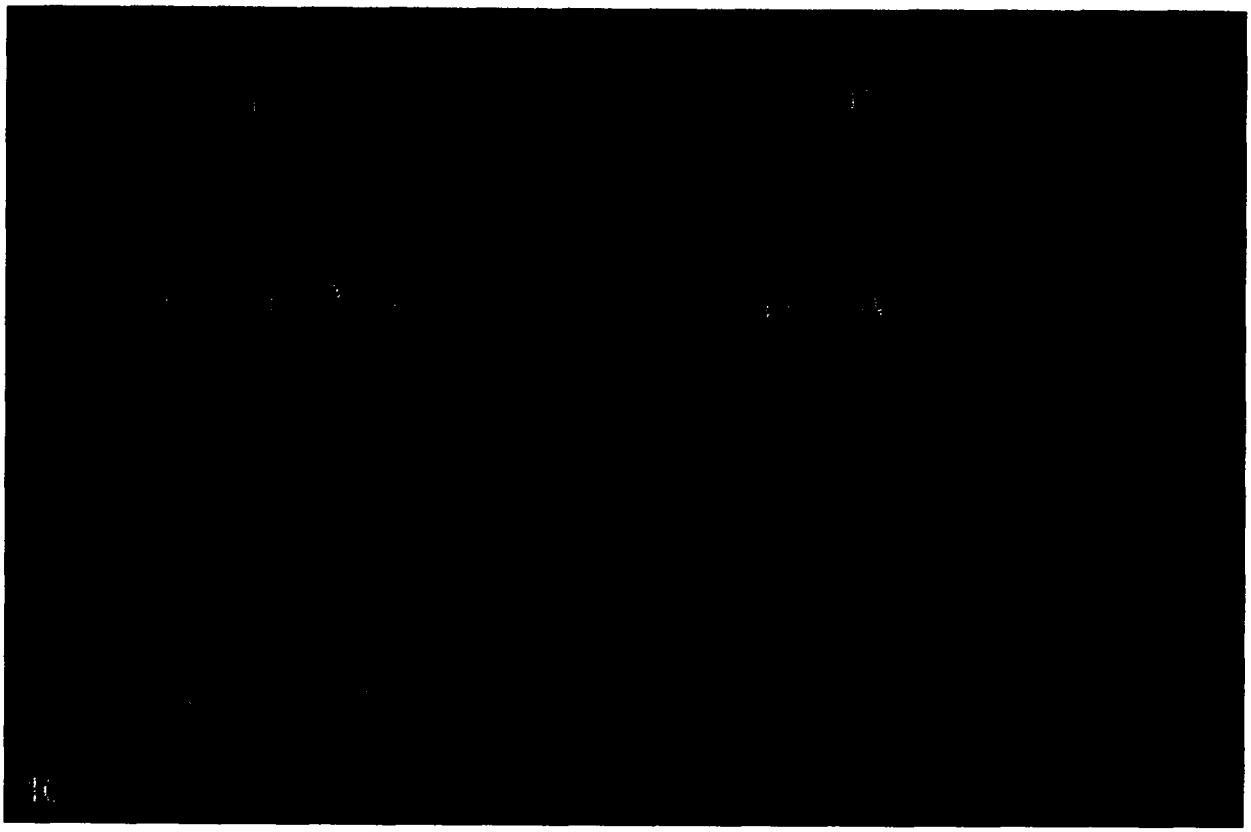

Figure 10. MI (left) and MP (right) conformations of pyrrolidinyl analogs **11** (top) and **12** (bottom). (A) MI conformation of **11** ($\omega_1 = 0°$, $\omega_2 = 71°$); (B) MP conformation of **11** ($\omega_1 = -55°$, $\omega_2 = 102°$); (C) MI conformation of **12** is high energy due to steric crowding between CH_2 and C=O ($\omega_1 = 96°$, $\omega_2 = -88°$); (D) MP conformation of **12** is lowest energy ($\omega_1 = 50°$, $\omega_2 = -102°$).

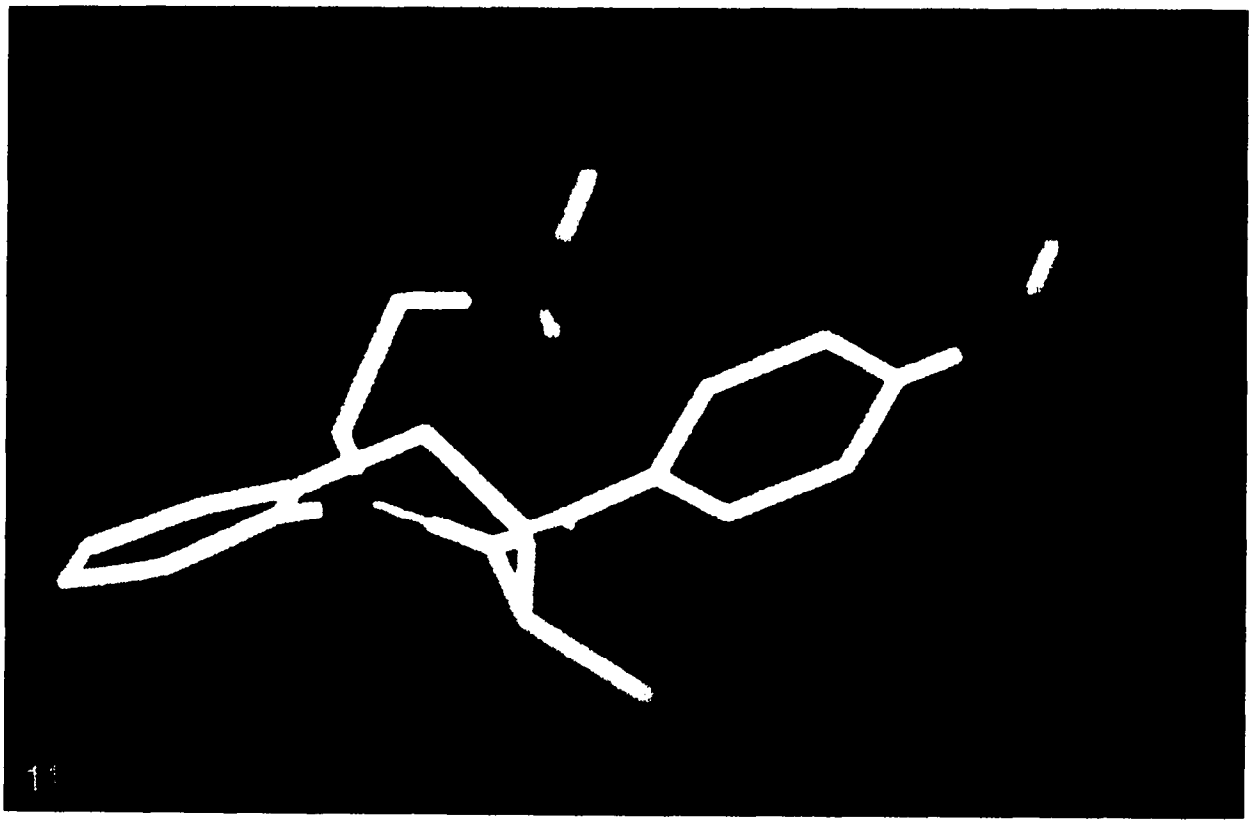

Figure 11. Model of bound conformation MI: benzazepinone **1a**

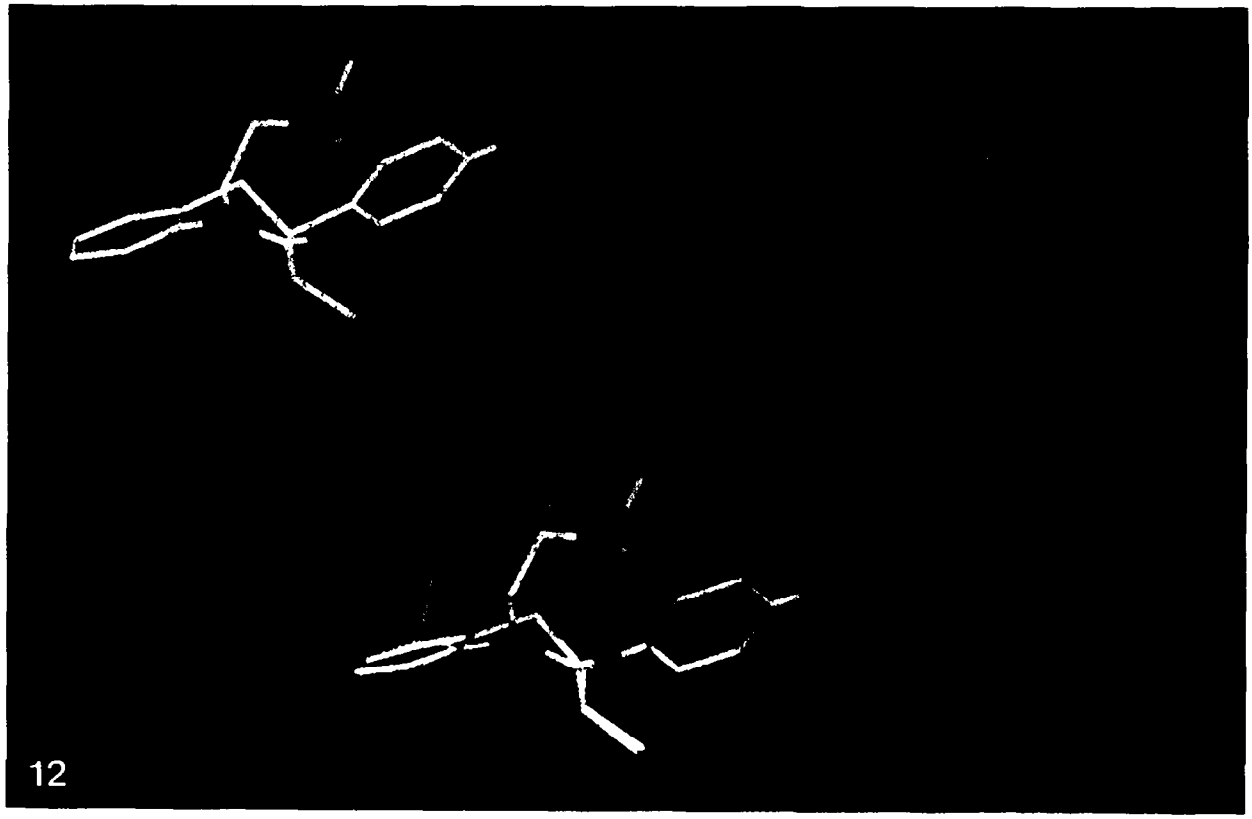

Figure 12. Model of bound conformation MI with benzazepinone **11**

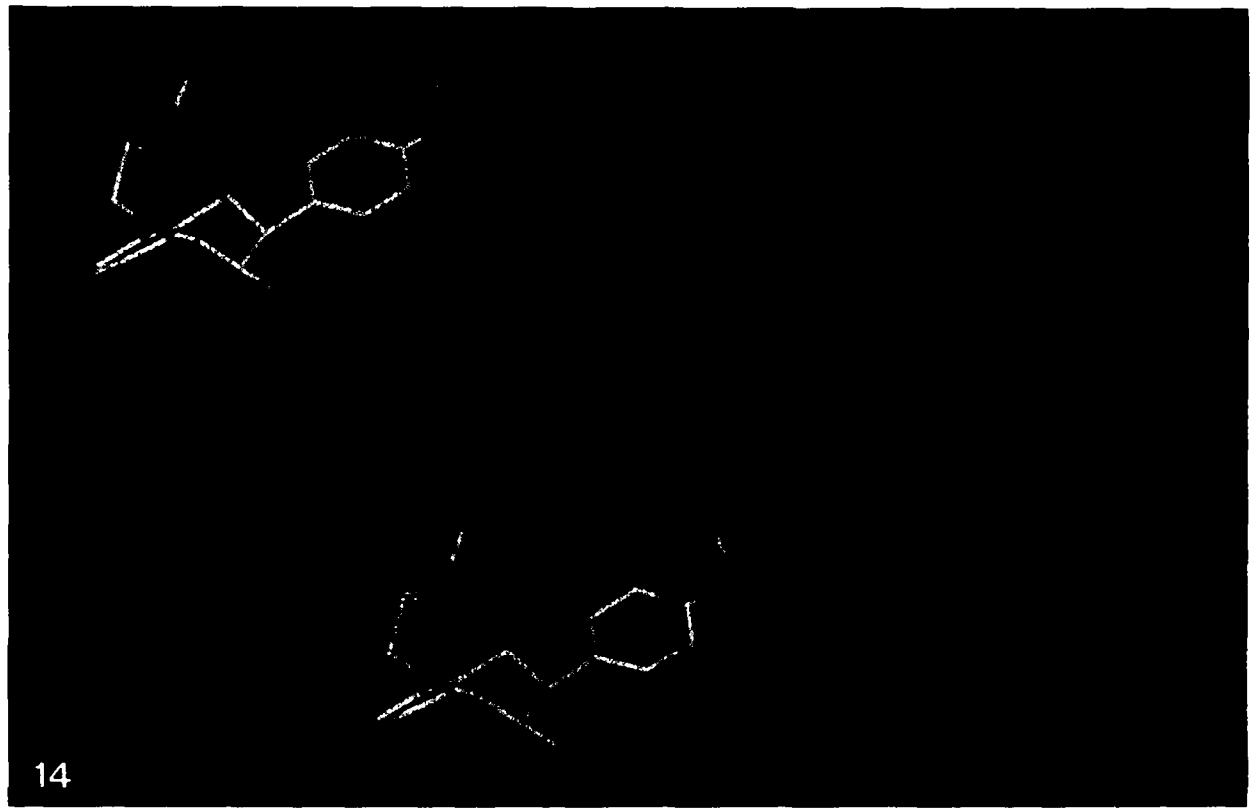

Figure 14. Model of bound conformation MI with desmethoxyverapamil **27b**

Cyclohexyl analog (8)

In contrast to compounds **3–5**, the introduction of a 1,2-*trans* disubstituted cyclohexane ring as a conformational constraint locks the dimethylamino ethyl substructure in an *sc* (ω_2) conformation with respect to the amide nitrogen. Figures 7, 8 and 9, illustrate the accessible low energy conformations for **8**. Figure 7 presents the observed solid state conformation of **8** (MO, ω_1 = -47°, ω_2= -49°), which clearly demonstrates the trans diequatorial substitution on the cyclohexane ring. Since there is only one rotatable bond between the benzazepinone ring and the basic sidechain, complete rotation of the basic nitrogen through ω_1 (Figure 8) maps out a circle, in contrast to the surface mapped out by benzazepinone **3**. Limiting the points on the circle to energetically accessible conformations for the basic nitrogen (within 10 kcal/mol of the minimum) provides Figure 9, in which there are far fewer possible conformations than with the unconstrained benzazepinone **3**.

The constrained benzazepinone **8** is a potent CCB, a fact which implicates a conformation close to one of those illustrated in Figure 9 as the receptor-bound structure. Furthermore, the fact that **8** is a potent calcium antagonist *in vitro* and *in vivo* virtually eliminates the possibility that an extended *ap* binding mode (ω_2 ~180°) is the unique bound conformation of these calcium antagonists.

However, it is important to take note of the fact that the activity of racemic **8** is five-fold less than racemic **3**. This data implies that the conformations attainable by the basic amine of **8**, while adequate for activity, may not be optimal.

Pyrrolidinyl analogs

The conformational analysis of cyclohexyl analog **8** strongly suggests that the bound conformation of benzazepinones is related to MI. In order to further refine this understanding we prepared 3-pyrrolidinyl substituted benzazepinones **11** and **12**, which differ only in the stereochemistry at the center of attachment to the pyrrolidine ring. These two analogs are very useful in our analysis of the receptor bound conformation, as **11** is active (IC_{50} = 0.32 μM) while **12** is relatively inactive (IC_{50} = 3.8 μM).

Our analysis of the conformational space accessible to these benzazepinone analogs (details not shown) indicated that, in addition to MI ("inboard") and MO ("outboard"), conformations MP (nitrogen near the plane of the lactam) may also be important. Figure 10 illustrates the MI and MP conformations for pyrrolidines **11** and **12**.

The MI and MP conformations for the active *R* pyrrolidine **11** are shown in Figures 10A and B, respectively. Our calculations show that both MI and MP conformations are energetically accessible for **11**. Figures 10C and D illustrate the MI and MP binding conformations of the inactive *S* pyrrolidine **12**. While the MP conformation represents the global minimum for **12** (Figure 10D), the MI orientation of the pharmacophores shown in Figure 10C is much higher in energy, due to steric repulsion between the methylene hydrogen and the amide carbonyl oxygen.

We reasoned that the difference in activity between these two pyrrolidines must be due to the conformational space that the analogs can occupy. In particular, **11** must have a low energy conformation that is close to the receptor-bound structure, while the analogous receptor-bound conformation for **12** must be less favorable. The comparison of compounds **11** and **12** illustrated in Figure 10 supports the hypothesis that MI is the conformation most relevant to receptor binding.

Computations and substituted analogs

In order to evaluate possible conformations of compounds **14**, **15**, **18**, **19**, **21**, and **22** (Tables 3 and 4), we carried out a Monte Carlo search using a constraint of 6.4–8.5 Å on the distance between the two pharmacophores. The results of these computations are shown in Table 4. For all of these compounds, an MI conformation is close to the global energy minimum. However, the MP conformation is *not* accessible to compounds **19**, **21**, and **22**. We believe that the good activity of **19**, **21**, and **22** as calcium channel blockers can only be ascribed to the ability of these compounds to bind in the MI conformation. The conformation–activity relationships obtained for this set of compounds are therefore consistent only with a receptor-bound conformation that approximates MI.

MI Model for Receptor Binding

The solid state conformation of **1a** serves as a model for the putative active conformation MI (Figure 11). The conclusion that MI represents the active conformation of diltiazem-like molecules is consistent with all of our previous SAR.[4] The positions of substitution that influence benzazepinone activity indirectly (e.g., through log *P* effects, Figure 2) are spatially remote from the region where the pharmacophores directly interact with the receptor. Figure 12 shows the active 3-pyrrolidinyl analog **11** in the calculated MI conformation overlaid with the MI receptor binding model.

In the conformation represented by MI, the two critical pharmacophores are positioned on the same face of the molecule, as if they were being presented together to the receptor. Interestingly, the relationship between the two critical pharmacophores in the MI binding model approximates 3-methoxy phenylethylamine. To the extent that MI represents the active conformation of benzazepinones and benzothiazepinones at the calcium channel binding site, these compounds may be seen as mimics of much smaller molecules. It is tempting to speculate that benzazepinones and benzothiazepinones may be serendipitously binding to a site normally occupied by an endogenous ligand (regulator) of the calcium channel. In our view, the benzazepinone ring of our compounds, and the benzothiazepinone ring of diltiazem, are serving as

Table 4. Preferred conformations of N1-substituted benzazepinones

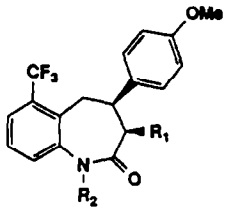

compd	R_1	R_2	conformer[a]	O-N distance (Å)[b]	relative E[c]
4	OAc		MI	7.4	1.2
			MP	8.1	2.7
5	OAc		MI	7.3	0.0
			MP	8.4	1.8
8	Me	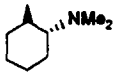	MP	9.1	0.0
			MI	7.1	5.9
11	OH (R)		MP	8.7	0.0
			MI	7.6	4.2
12	OH (S)		MP	8.3	0.0
14 (isomer A) OH (calculated as R isomer)		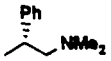	MP	8.2	0.0
			MI	7.2	0.6
			MI	7.3	4.4
			MP	8.4	5.1
15 (isomer B) OH (calculated as S isomer			MI	7.6	0.1
			MI	8.1	1.6
			MI	7.6	1.9
			MP	7.6	3.2
18 (1R,2R) OH			MP	8.3	0.4
			MI	7.1	1.8
			MI	7.6	5.6
19 (1S,2R) OH			MI	8.0	0.0
			MI	8.4	1.5
			MI	7.5	4.4
21 (1R,2S) OH		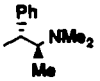	MI	8.4	0.0
			MI	7.6	3.0
22 (1S,2S) OH		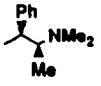	MI	7.7	0.0
			MI	8.1	4.7

[a]Conformer pattern MI ("inboard") or MP ("in plane"); see text.
[b]Distance between pharmacophores; see Figure 2.
[c]Energy relative to global minimum in kcal/mol.

scaffolding, and function primarily to position the basic amine pharmacophore with respect to the aryl methyl ether.

Supportive evidence for MI: SAR of amino substitution

Further evidence in support of binding model MI is provided by benzazepinone analogs in which the basic amino group is substituted by groups larger than methyl (Table 5). Increasing bulk around the basic amino group is deleterious to activity, in spite of the beneficial effect that increasing log *P* has on activity *in vitro*.[4] The activity in the series **3**, **23**, **24** decreases in proportion to the bulk introduced around the basic nitrogen. Benzazepinones in which the basic amine is part of a ring (**25**) are also much less active. These findings are also consistent with binding mode MI. Substitution at the basic nitrogen will provide a steric impediment that should interfere with the binding of the basic amino group in the MI conformation. In the MI conformation, these bulky alkyl groups will be on the β face of the molecule, hindering the interaction of the basic amino pharmacophore with the calcium channel protein. Alternatively, increasing the bulk around the basic nitrogen might favor an extended MO conformation, which should also decrease activity.

Possible Relationship to Desmethoxyverapamil

At least three distinct classes of calcium channel blockers have been described in the literature: the dihydropyridines (DHP) **26**, phenylalkylamines (PA) **27**, and diltiazem-like compounds such as benzazepinone **3** (DTZ).[14] Figure 13 shows a generally accepted model for interactions between their binding sites on the calcium channel.[15] The nature of the allosteric interactions between different CCBs is complex and highly dependent upon tissue and experimental conditions. However, the dihydropyridines (DHP) are easily differentiated from the other classes of CCBs, both structurally as well as by their binding site.[16] The dihydropyridine binding site is distinct from the phenylalkylamine and diltiazem binding sites;[17] DHP binding is decreased by PAs, while DTZ typically increases binding of DHPs. In contrast, DTZ is a negative allosteric regulator of PA binding, and *vice versa*.

The relationship between the DTZ and PA binding sites remains ambiguous, but the weight of current evidence points towards different binding sites for these two classes of compounds.[17,18]

Table 5. Activity of racemic N1 substituted benzazepinones *in vitro*

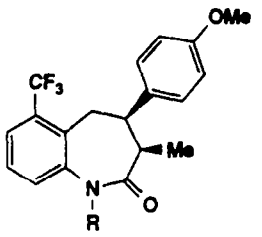

compd	R	log P (est'd)[a]	IC_{50}(μM)[b]	kd (μM)[c]
3		3.6	0.076 (0.041-0.14)	0.075 ± 0.043
23	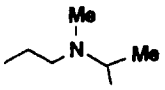	3.8	0.81 (0.38-1.7)	0.13 (+0.014)
24	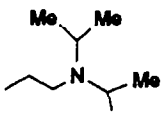	4.0	4.2 (2.5-6.8)	-
25	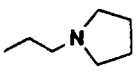	3.9	1.1 (0.52-2.4)	66% (1 μM)

[a]Log *P* estimated by reverse phase HPLC.[4]
[b]IC_{50} in rabbit aorta strips contracted with KCl (95% confidence interval).
[c]k_d Determined by displacement of radiolabeled diltiazem in guinea pig striated muscle (± SEM).

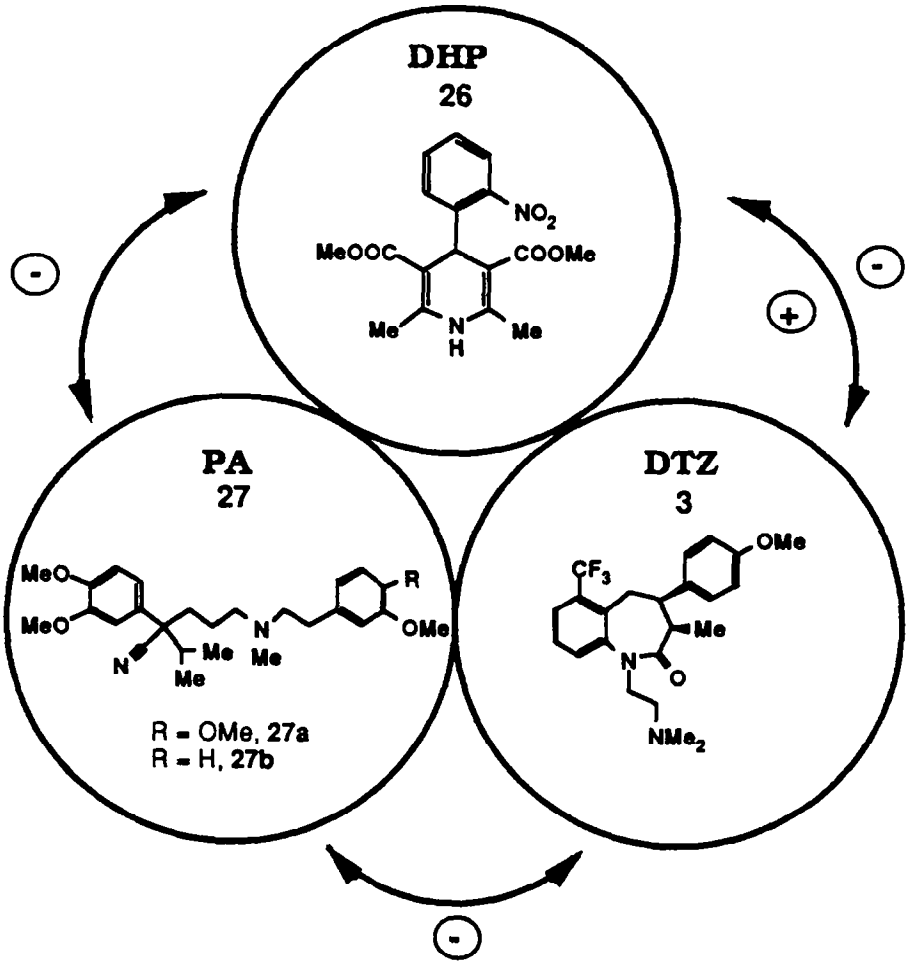

Figure 13. Allosteric interactions of calcium channel blockers

Desmethoxyverapamil (**27b**) has found wide experimental application as a prototype phenylalkylamine. This compound contains the 3-methoxy phenylethylamine substructure of the MI binding model for diltiazem-like compounds. It differs from verapamil **27a** by the deletion of a single methoxy substituent on the aryl ring of the 3,4-dimethoxy phenylethylamine substructure (see Figure 13).

Depending upon the experimental conditions, desmethoxyverapamil has demonstrated molecular pharmacology typical of either PAs or DTZ. Numerous experiments have indicated that desmethoxyverapamil behaves as a classical phenylalkylamine CCB in its interaction with DHPs.[19] However, **27b** has also been shown to potentiate the binding of antagonist dihydropyridines, and decrease the binding of agonist dihydropyridines,[20] allosteric interactions suggestive of DTZ-like binding. Other workers have concluded that **27b** labels *both* PA and DTZ sites in brain and skeletal muscle.[21]

We believe that the SAR of benzazepinone CCBs, and the evidence for the MI binding mode, further supports the possibility that **27b** can bind at *either* the PA binding site or the DTZ binding site on the α1 subunit of the calcium channel. In Table 6 we compare the activity of the benzazepinone **3** with its 3',4'-dimethoxy congener **28**. In the MI binding mode, the pharmacophores of these compounds would fit in the same manner as 3-methoxy phenylethylamine and 3,4-dimethoxy phenylethylamine, respectively. From its poor activity, the dimethoxy-substituted **28** must *not* fit at the DTZ receptor. Since it is an extremely weak CCB, it apparently also lacks the structural prerequisites for the PA receptor. Compounds **3** and **28** contain the substructures of desmethoxyverapamil (**27b**) and verapamil (**27a**), respectively. Whereas we might expect **27b** to bind to the DTZ receptor in the MI mode via its 3-methoxy phenylethylamine substructure, **27a** (in analogy with **28**) should bind poorly. Thus, the small structural alteration between **27a** and **27b** might be highly significant in terms of their relative ability to interact with the DTZ receptor on the calcium channel. The fit of desmethoxyverapamil to the benzazepinone binding model MI is shown in Figure 14.

Table 6. Comparison of racemic 4-aryl substituted benzazepinones in vitro

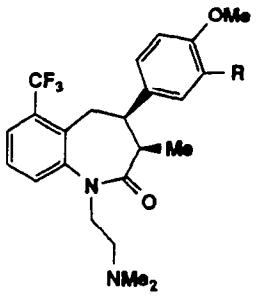

compd	R	log P (est'd)[a]	$IC_{50}(\mu M)$[b]	kd (μM)[c]
3	H	3.6	0.076 (0.041-0.14)	0.075 ± 0.043
28	OCH_3	2.9	3.8 (1.9-7.5)	2.0 ± 0.83

[a]Log *P* estimated by reverse phase HPLC.[4]
[b]IC_{50} in rabbit aorta strips contracted with KCl (95% confidence interval).
[c]k_d Determined by displacement of radiolabeled diltiazem in guinea pig striated muscle (± SEM).

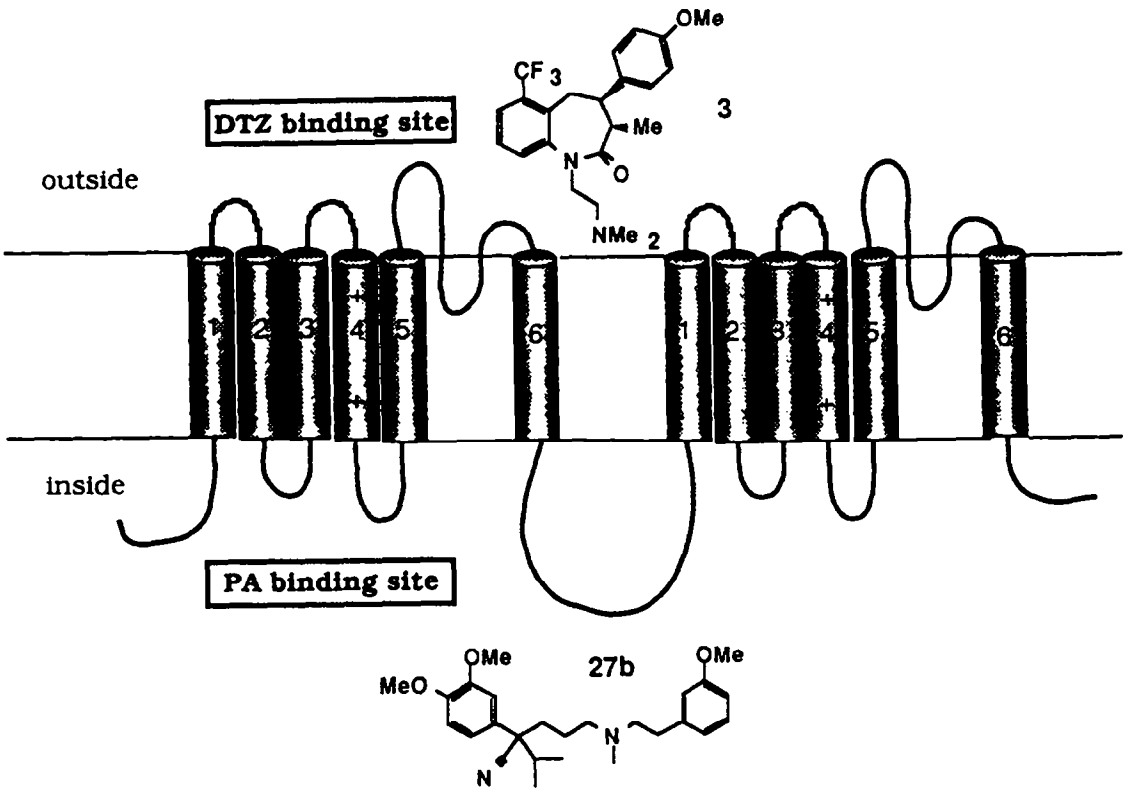

Figure 15. Postulated locus of binding sites on α1 subunit

It has been established through electrophysiological experiments that the PA binding site is on the cytoplasmic face of the cell membrane.[22] Analogous studies with a quaternary benzazepinone have demonstrated experimentally that the DTZ binding site must be accessible from the extracellular face of the calcium channel protein.[18b] Figure 15 is a cartoon of the putative binding sites for the PA and DTZ classes of calcium channel blockers. If our hypothesis is valid that **27b** binds to both the DTZ and the PA binding sites, then a quaternary analog of desmethoxyverapamil should be able to block channels selectively at either site if delivered intracellularly (PA site) or extracellularly (DTZ site). Experiments to test this prediction are in progress.

Conclusions

We have studied the structure–activity relationships of several conformationally constrained benzazepinones calcium channel blockers. From this work, the binding conformation of benzazepinone and benzothiazepinone (e.g.

diltiazem) CCBs is best described by the MI binding model. This binding model places both the amine and phenyl methyl ether pharmacophores on the β face of the molecule in close apposition. This model of the receptor-bound conformation of DTZ-like calcium channel blockers implies that both diltiazem and the benzazepinone CCBs are relatively complicated structures that deliver a simple 3-methoxy phenylethylamine substructure to a binding site on the calcium channel protein. Our working hypothesis that MI represents the active, bound conformation of benzazepinones is consistent with all previous SAR of these compounds.[2-5] Further, this binding hypothesis suggests that desmethoxyverapamil **27b** may be able to bind at both the DTZ site and the PA site on the calcium channel.

Based upon these findings we hypothesize that benzazepinone and benzothiazepinone CCBs consist mostly of "scaffolding" that serves to orient the two pharmacophores in space. We have no reason to believe that this structural arrangement is optimal. Indeed, it is also conceivable that this structural scaffolding sterically hinders receptor access and limits the activity of DTZ-like compounds. From this vantage point, altering the scaffolding that constrains the two key pharmacophores could provide compounds of equal or greater intrinsic potency than the benzazepinone or benzothiazepinone CCBs. Thus, we believe that the greatest benefit from formulating receptor binding hypothesis MI will be in its ability to guide the *de novo* design of structurally unique CCBs. Our initial attempts to use this working hypothesis in the design of novel organic ligands for the DTZ site is described in the following paper in this series.

Experimental Section

Pharmacological testings

The pharmacological test procedures have been described in detail in a previous paper in this series.[2] The IC_{50} value reported represents the concentration of compound necessary to cause 50% relaxation of a maximal contraction (circumferential rabbit aorta strips) in response to 100 mM KCl. The k_d values reported were calculated from concentration response curves for the inhibition of specific ^3H–diltiazem binding in guinea pig skeletal muscle. We have published previously correlations between the SAR of benzothiazepinones and benzazepinones,[2] and have found that the slope factors are > 0.77 for all compounds in this paper. These results are consistent with a competitive displacement of ^3H–diltiazem by the test compounds.

Computational chemistry

Torsional grid search. Torsional grid scans were examined graphically, using the interactive crystallographic/molecular modeling software, ALEX, developed in-house by JZG. Tandem rotations of 360° in 10° increments for ω_1 and ω_2 (1296 conformers) were scanned, for a fixed "M" twist-boat conformation. All bond distances and angles were held fixed throughout the torsional scans. The nonbonded interactions of each conformer were estimated using a 6,12 potential. Coulombic interactions were ignored. More refined calculations were performed using molecular mechanics software.

Macromodel/Monte Carlo. The grid searches and Monte Carlo searches for the compounds in Table 4 were carried out using Macromodel and the MM2 force field within Macromodel. Sybyl was employed for the graphical analysis and molecular constructions. In addition, Csearch (Sybyl) was employed to carry out a conformational search of the sterically accessible torsional space for verapamil (**27a**).

Although the compounds of Table 4 differ in their R_1 substituent, for computational purposes they were all modeled with a methyl group at R_1. The 4'-OMe group was also converted to a methyl group to simplify computations. The starting structures for all the molecules of Table 4 were constructed from the crystal structures of **3** and **8** by modifying and appending different functionalities. The "M" conformation of the benzazepinone ring was assumed for all compounds.[1]

Searches were carried out for both pseudoaxial and pseudoequatorial orientations of compounds **11** and **12**. A grid search about the free torsional angles of interest was carried out using an increment of 5 degrees. All conformers within 6 Kcal of the minima were compared to determine the low energy families of conformations common to **8** and **11** but inaccessible to **12**. The conformation that was found corresponded to binding mode MI. This conformation had a distance between the basic nitrogen and the methoxy oxygen (represented computationally by carbon) of 7.1 Å and 7.6 Å for **8** and **11**, respectively. A distance range constraint of 6.4–8.5 Å was then used in Monte Carlo searches for conformers of the remaining molecules **4, 5, 14, 15, 18–22**. Only conformers within 6 Kcal of the global minimum for this constrained search were kept.

Three-dimensional pharmacophore search. A search of all crystal structures in the Cambridge Structural Database[23] for molecules containing functional groups in spatial relationships consistent with a set of postulated pharmacophores was conducted using a series of local[24] FORTRAN software programs. The database was initially screened using the distributed[23] CONNSER software for all entries containing: (a) a benzene ring with at least two substituents—a heteroatom *para* to a carbon substituent, and (b) an N–CH_3 bond within the same molecule. All structures satisfying this substructure query were further screened with the geometric constraints: (a) a distance of 7.5±1.0 Å from the nitrogen atom to the carbon atom, C4, bearing the heteroatom X, and (b) a value of 110 ± 40° for the X–C4....N angle. Since it was impractical to evaluate the geometric constraints through manual inspection of each of the many hits of the initial substructure query, subroutines were written to automatically perform the structure retrieval–geometric evaluation process. It was

first necessary, however, to canonically reorder the entire database in order to obtain the correspondence between the atoms of the substructure search and the atoms in the arrays of observed atomic coordinates. ("Matching integers" which define this correspondence have become available in more recent releases of the database.)

Structures satisfying the geometric constraints were examined using local graphics software (ALEX) which executes a three-dimensional least squares superposition of the query atoms prior to display. The spatial similarity of the postulated pharmacophores in the benzazepinone and verapamil (CSD refcode = CURHOM[25]) structures was first recognized in this manner.

Crystallographic studies

Crystal data and some details of the structure refinements are given in Table 7. Unit cell parameters were obtained through least-squares analysis of the experimental diffractometer settings of 15 high-angle reflections. Crystal densities were measured by flotation methods. Intensities were measured diffractometrically using Cu Kα radiation (λ = 1.5418 Å) at 23°C with the θ-2θ variable scan technique and were corrected only for Lorentz-polarization factors. Background counts were collected at the extremes of the scan for half of the time of the scan. The structures were solved by direct methods[26] and refined on the basis of observed reflections [$I \geq 3\sigma(I)$], using the SDP[27] software package. Least-squares weights $w = \sigma^{-2}(F_o)$ were calculated with the assumption that $\sigma^2 = \varepsilon^2 + (pI)^2$ where ε is the statistical counting error and $p = 0.02$–0.04. The function minimized in the least-squares refinements is $\Sigma_w(|F_o| - |F_c|)^2$. R is defined as $\Sigma\, ||F_o| - |F_c||/\Sigma\, |F_o|$ while R_w is defined as $[\Sigma_w (|F_o| - |F_c|)^2/\Sigma_w |F_o|^2]^{1/2}$. Most hydrogen positions were evident during the latter stages of refinement. All hydrogens on carbon were introduced in idealized positions; those on heteroatoms were introduced only if they were observed on difference maps. Although the scattering of hydrogens was included in the terminal stages of refinement, no hydrogen parameters were varied. Final difference maps contained no significant features.

General chemical procedures.

Melting points were recorded on a Thomas-Hoover capillary apparatus and are uncorrected. Proton NMR (^{1}H NMR) spectra were obtained on JOEL FX-270 or GX-400 spectrometers and are reported relative to tetramethylsilane (TMS) reference. Carbon NMR (^{13}C NMR) data were obtained on the JOEL FX-270 or FX-60Q spectrometers and are also reported relative to TMS. Optical rotations were recorded with a Perkin-Elmer 241 spectrophotometer. All reactions were conducted under an atmosphere of dry nitrogen or argon using anhydrous solvents unless noted otherwise.

[1(trans),3α,4α]-1-[2-(Dimethylamino)cyclohexyl]-1,3,4,5-tetrahydro-4-(4-methoxyphenyl)-3-methyl-6-trifluoromethyl-2H-1-benzazepin-2-one (8)

To a suspension of 0.3 g of NaH (6.3 mmol of a 50% oil dispersion) in dry DMF (20 mL) was added **6** (2.0 g, 5.73 mmol) in one portion as a solid. The solution was stirred for 45 min and a solution of *trans*-β-iodo-dimethylaminocyclohexane **7**[10] (1.6 g, 6.3 mmol) in dry DMF (12 mL) was added dropwise over 15 min. The solution was stirred at r.t. for 20 min and then heated to 75 °C for 70 min. Additional NaH (0.15 g) and **7** (0.8 g, 3.2 mmol) were added and heating was continued for an additional 30 min. The solution was allowed to cool and the DMF was removed *in vacuo*. Water was added to the residue, the aqueous solution was extracted twice with ethyl acetate and the combined organic phases were washed with brine and dried ($MgSO_4$) to afford 3.15 g of semi-solid. Chromatography (SiO_2; 1% Et_3N:2% MeOH:CH_2Cl_2) afforded the free base as a foamy colorless solid (0.74 g, 27%). The free base was dissolved in ether and ethereal HCl was added to afford a colorless precipitate, which was washed twice with ether to remove excess HCl. The remaining solid was recrystallized from *i*PA–*i*PE to afford **8** (0.68 g, 23%). m.p. > 250 °C. $(M + H)^+ = 475$. IR ($CHCl_3$): 1650 cm^{-1}. Anal. ($C_{27}H_{33}F_3N_2O_2$·HCl) C, H, N, Cl, F. ^{1}H NMR (CD_3OD): δ 0.71 (d, 3H, J = 6.3) 1.30 (m, 1H), 1.53 (m, 2H), 1.82 (d, 1H, J = 13.7), 1.94 (m, 2H), 2.29, (m, 2H), 2.66 (m, 1H), 2.99 (s, 3H), 3.05 (s, 3H), 3.21 (m, 2H), 3.79 (s, 3H), 3.86 (m, 1H), 4.93 (m, 1H), 6.91 (d, 2H, J = 8.4), 7.15 (d, 2H, J = 8.4), 7.52 (d, 1H, J = 7.9), 7.64 (t, 1H, J = 7.9), 7.75 (d, 1H, J = 7.4). ^{13}C NMR (CD_3OD): δ 14.1, 25.4, 25.7, 30.4, 35.8, 35.9, 38.1, 41.2, 44.3, 53.4, 55.7, 67.1, 68.5, 114.9, 126.2, 130.4, 131.2, 134.2, 136.3, 145.5, 160.4, 179.0 ppm.

[3R-[1(R),3α,4α]-1,3,4,5-Tetrahydro-3-hydroxy-4-(4-methoxyphenyl)-1-(3-pyrrolidinyl)-6-trifluoromethyl-2H-1-benzazepin-2-one (11)*

A mixture of *N*-benzyl-3(*S*)-tosyl-pyrrolidine **10** (2.2 g, 6.64 mmol), compound **9** (1.86 g, 5.31 mmol) and Cs_2CO_3 (8.65 g, 26.5 mmol) was heated to reflux in MEK (75 mL) for 18 h. The reaction was cooled, diluted with ether (150 mL), and filtered through celite. The filtrate was concentrated and the residue was chromatographed (SiO_2; EtOAc:hexane 3:1, then MeOH:CH_2Cl_2 1:40) to provide the *N*-benzyl derivative (1.64 g, 61 %).

The *N*-benzyl derivative (1.58 g, 3.1 mmol) was dissolved in glacial acetic acid (30 mL) and hydrogenated (500 mg of 20% $Pd(OH)_2$/C) for 3 h at r.t. The reaction was filtered through celite and the filter cake washed with glacial acetic acid (15 mL). The filtrate was diluted with water (150 mL) and the solution was made basic with solid Na_2CO_3, extracted with EtOAc (150 mL), washed with brine and dried ($MgSO_4$). The filtrate was concentrated and chromatographed (SiO_2, packed with 1% Et_3N; 5% MeOH: CH_2Cl_2 to 10% MeOH: CH_2Cl_2) to provide the free base as a colorless foam (1.17 g). The free base (1.08 g, 2.57 mmol) was dissolved in MeOH and fumaric acid (298 mg, 2.57 mmol) was added as a solution in hot MeOH. The resulting solution was concentrated to a colorless foam, crystallized from *i*PA, filtered, and dried *in vacuo* to provide **11** as a crystalline solid (925 mg, 68%). m.p. 214–216 °C. $[\alpha]_D^{25} = +58.9°$ (c = 0.50, MeOH). (M +

Table 7.

Compound	4	8	9	Ref 5, 5c	Ref 5, 5c[d]	Ref 5, 5d[d]	Ref 2, 15m	Ref 2, 14m	Ref 2, 12m
Solvent	S-2 BuOH/ MeCN	MeCN/ether		$CDCl_3$, DMSO-d_6; $CHCl_3$	MeCN/H_2O	MeCN/H_2O	ether	hexane	
a, Å	12.711(4)	24.904(2)	15.061(1)	8.873(1)	8.530(1)	8.619(1)	16.947(2)	19.60(2)	10.365(2)
b, Å	7.697(2)	11.122(1)	27.684(2)	38.054(3)	43.833(5)	43.186(6)	14.21(1)	13.916(9)	13.149(1)
c, Å	12.889(3)	19.042(2)	7.825(2)	7.281(1)	7.274(1)	7.402(1)	9.134(4)	10.574(5)	15.690(2)
β°	96.48(2)								
V, Å3	1253(1)	5274(2)	3263(1)	2458.6	2720(1)	2755(1)	2199(5)	2884(6)	2138.3(8)
Space Group	$P2_1$	$Pca2_1$	$P2_12_12_1$	$P2_12_12_1$	$P2_12_12_1$	$P2_12_12_1$	$P2_12_12_1$	$P2_12_12_1$	$P2_12_12_1$
Formula	$C_{25}H_{27}N_2O_4F_3Cl$	$C_{27}H_{33}N_2O_2F_3 \cdot HCl$	$C_{18}H_{16}NO_3F_3$	$C_{25}H_{31}N_2O_5Cl$	$C_{25}H_{31}N_2O_5Cl \cdot CH_3CN$	$C_{24}H_{29}N_2O_5SCl \cdot CH_3CN$	$C_{23}H_{25}N_2O_4F_3$	$C_{26}H_{26}N_2O_6F_3Cl_3$	$C_{22}H_{25}N_2O_3F_3$
FW	511.95	510.0	351.3	474.98	516.04	534.08	449.5	635.9	422.5
Z	2	8	8	4	4	4	4	4	4
d_{obs}, g-cm^{-3}	not measured	1.28	1.42	1.29	1.26	1.27			1.30
d_{calc}, g-cm^{-3}	1.357	1.285	1.43	1.283	1.27	1.29	1.36	1.44	1.312
NUNI[a]	2029	5164	3647	2701	3007	3024	2137	3029	2277
NOBS[b]	551	3659	1580	1989	2581	2271	883	1432	1523
NV[c]	145	631	452	299	326	326	129	362	247
R	0.072	0.045	0.049	0.048	0.052	0.054	0.087	0.064	0.11
R_w	0.077	0.052	0.052	0.059	0.067	0.064	0.087	0.068	0.13

[a]Number of symmetry-independent reflections.
[b]Number of observed reflections with $I \geq 3\sigma(I)$ used in least-squares refinements.
[c]Number of refined variables.
[d]As a clear demonstration of molecular isosterism, **5c** and **5d** have been found to be crystallographically isostructural. The molecular packing of **5d** requires only 1.3% greater volume than **5c**.

H)$^+$ = 421. IR (KBr): 3430, 1513. Anal. ($C_{22}H_{23}F_3N_2O_3 \cdot C_4H_4O_4$) C, H, N, F. ^{1}H NMR (DMSO-d_6): δ 2.33 (m, 2H), 3.00 (d, 2H, J = 10), 3.11 (m, 1H), 3.46 (m, 3H), 3.73 (s, 3H), 3.68–3.76 (m, 1H), 4.00 (d, 1H, J = 8), 4.59 (m, 1H), 6.44 (s, 2H), 6.87 (d, 2H, J = 9), 7.15 (d, 2H, J = 9), 7.60 (m, 1H), 7.69 (m, 2H). ^{13}C NMR (DMSO-d_6): δ 29.0, 32.4, 44.3, 46.8, 51.1, 55.0, 60.2, 68.8, 113.4, 124.2, 128.1, 128.6, 129.6, 131.4, 132.7, 135.0, 143.2, 158.2, 168.0, 171.8.

[3R-[1(S),3α,4α]-1,3,4,5-Tetrahydro-3-hydroxy-4-(4-methoxyphenyl)-1-(3-pyrrolidinyl)-6-trifluoromethyl-2H-1-benzazepin-2-one (12).*

m.p. 228–231 °C. $[\alpha]_D^{25}$ = +57.8° (c = 1.0, HOAc). (M + H)$^+$ = 421. IR (KBr): 3513, 1660, 1513. Anal. ($C_{22}H_{23}F_3N_2O_3 \cdot C_4H_4O_4$) C, H, N, F. ^{1}H NMR (DMSO-d_6): δ 2.21 (m, 1H), 2.45 (m, 1H), 2.99 (m, 2H), 3.17 (m, 1H), 3.49 (m, 2H), 3.56 (d, 2H, J = 7.5), 3.75 (s, 3H), 4.03 (d, 1H, J = 7.5), 4.65 (m, 1H), 6.48 (s, 2H), 6.88 (d, 2H, J = 8), 7.17 (d, 2H, J = 9), 7.60 (t, 1H, J = 8), 7.71 (t, 2H, J = 7.5). ^{13}C NMR (DMSO-d_6): δ 28.5, 32.3, 44.7, 47.4, 51.2, 55.0, 60.0, 68.9, 113.4, 124.2, 128.1, 129.6, 131.4, 132.7, 135.0, 143.1, 158.2, 167.9, 171.9.

(3R-cis)-1-[2-(Dimethylamino)-1-phenylethyl]-1,3,4,5-tetrahydro-3-hydroxy-4-(4-methoxyphenyl)-1-(3-pyrrolidinyl)-6-trifluoromethyl-2H-1-benzazepin-2-one isomer A (14)

To a stirred suspension of NaH (0.75 g, 15.6 mmol of 50% oil dispersion) in dry DMF (30 mL) was added **9** (5.0 g, 14.2 mmol) in one portion as a solid. The solution was stirred for 1 h at r.t., heated to 70 °C, and a toluene solution of *N,N*-dimethyl-β-chloro-phenethylamine **13** was added dropwise over 2 h.[12,13] An additional aliquot of **13** (4.5 mmol) was added after 2 h, and the resulting solution was stirred at 70 °C for 2 h, and then quenched with aqueous $NaHCO_3$. The solvents were removed *in vacuo*, the residue partitioned between EtOAc and aqueous $NaHCO_3$, the organic phase washed with brine, dried ($MgSO_4$), filtered, and evaporated to afford a light yellow gum. The crude product was chromatographed (SiO_2; 2% MeOH:0.5% Et_3N:CH_2Cl_2) to provide the pure FMI (faster moving isomer) as a light yellow foamy solid (1.90 g, 27%). A solution of the clean FMI (0.41 g) in ether was treated with ethereal HCl, the resulting solid filtered, rinsed with ether and dried. This material was dissolved in *i*PA (2 mL) and *i*PE (6 mL) with warming and the solution filtered to remove a small amount of insoluble material. The filtrate was treated with hexane and the resulting colorless solid collected by filtration and dried to afford **14** (0.39 g). m.p. 136–142 °C. $[\alpha]_D^{25}$ = +146.2° (c = 1.0, MeOH). (M + H)$^+$ = 499. IR (KBr): 1669 cm^{-1}. Anal. ($C_{28}H_{29}F_3N_2O_3 \cdot HCl$) C, H, N, Cl, F. ^{1}H NMR ($CDCl_3$): δ 1.94 (dd, 1H, J = 13.5, 14.1), 2.50 (d, 3H, J = 3.5), 2.80 (dd, 1H, J = 5.9, 14.1), 2.96 (d, 3H, J = 2.9), 3.50 (m, 1H), 3.79 (s, 3H), 4.06 (d, 1H, J = 8.2), 4.32 (d, 1H, J = 14.1), 4.58 (m, 1H), 5.63 (d, 1H, J = 7.0), 6.70 (d, 2H, J = 8.8), 6.76 (d, 2H, J = 8.8), 7.38–7.50 (m, 6H), 8.67 (m, 1H). ^{13}C NMR ($CDCl_3$): δ 30.5, 42.8, 45.4, 52.0, 55.2, 60.0, 65.0, 69.1, 113.5, 125.4, 128.0, 129.0, 129.4, 129.9, 130.1, 133.2, 142.1, 159.0, 173.3.

(3R-cis)-1-[2-(Dimethylamino)-1-phenylethyl]-1,3,4,5-tetrahydro-3-hydroxy-4-(4-methoxyphenyl)-1-(3-pyrrolidinyl)-6-trifluoromethyl-2H-1-benzazepin-2-one, isomer B (15).

Fractions from the chromatography of **14** containing SMI (slow-moving isomer) were pooled to provide 3.40 g of crude SMI. This material was chromatographed twice (SiO_2; 2% MeOH: 0.5% Et_3N:CH_2Cl_2, then preparative TLC 5% MeOH:CH_2Cl_2) to provide the pure free base (0.41 g), which was dissolved in ether and treated with ethereal HCl. The resulting colorless solid was filtered, rinsed twice with ether and dried to afford **15** (0.42 g).

m.p. 165–171 °C. $[\alpha]_D^{25}$ = +221.8° (c = 1.0, MeOH). (M + H)$^+$ = 499. IR (KBr): 1671 cm^{-1}. Anal. ($C_{28}H_{29}F_3N_2O_3 \cdot HCl$) C, H, N, Cl, F. ^{1}H NMR ($CDCl_3$): δ 2.45 (dd, 1H, J = 13.5, 14.1), 2.9–3.1 (m, 2H), 2.95 (s, 3H), 3.02 (d, 3H), 3.51 (m, 1H), 3.80 (s, 3H), 4.03 (m, 1 H), 4.2 (m, 1H), 4.23 (d, 1H, J = 8.2), 6.57 (m, 1H), 6.90 (d, 2H, J = 8.2), 7.16 (d, 2H, J = 8.8), 7.16–7.27 (m, 5H), 7.43 (t, 1H, J = 7.6), 7.55 (d, 1H, J = 7.6), 7.79 (d, 1H, J = 7.6), 12.05 (brs, 1H). ^{13}C NMR ($CDCl_3$): δ 31.8, 43.2, 45.2, 51.4, 55.3, 55.6, 60.0, 69.5, 113.9, 127.7, 128.5, 129.0, 129.6, 129.8, 130.2, 134.2, 139.0, 159.1, 174.5.

(3R)-1,3,4,5-Tetrahydro-3-tertbutyldimethylsiloxy-4-(4-methoxyphenyl)-6-trifluoromethyl-2H-1-benzazepin-2-one (16)

To a stirred solution of **9** (10 g, 28.5 mmol) and imidazole (4.85 g, 71.2 mmol) in dry DMF (10 mL) at 35 °C was added *t*-butyldimethylsilyl chloride (5.10 g, 33.8 mmol). The solution was stirred at 35 °C overnight, cooled to r.t., and partitioned between ether and water. The organic phase was washed with water and brine, dried ($MgSO_4$) and evaporated to afford **16** (14.20 g, 100%) as an amorphous solid. m.p. 114–116 °C. ^{1}H NMR ($CDCl_3$): δ 0.05 (s, 6H), 0.75 (s, 9H).

(1R,2R)-2-(Dimethylamino)-1-chloro-1-phenylpropane, hydrochloride (17)

To a suspension of 1*S*,2*R*-(+)-norephedrine hydrochloride (20 g, 106 mmol) in ether (50 mL) was added sodium methoxide in MeOH (100 mmol). Additional methanol (50 mL) was added, the solution stirred for several minutes and filtered. The colorless precipitate was rinsed several times with ether and the combined filtrates were evaporated to afford the free base as a colorless oil (16.6 g, 100%). The free base was dissolved in CH_3CN (125 mL) and aqueous formaldehyde (42 mL of 37%) was added. Sodium cyanoborohydride (10.5 g, 167 mmol) was added portionwise with intermittent cooling in an ice bath. Glacial HOAc was added to the cooled reaction until the pH of the solution dropped to 8, the solution was stirred at r.t. for 30 min and evaporated. The residue was partitioned between 2N NaOH and ether (3) and the combined ether layers washed with 0.5N NaOH, and extracted with 10%

HCl (3). The combined acid washes were neutralized with solid NaOH and extracted with ether (3), washed with brine, dried (K_2CO_3) and evaporated to afford the *N,N*-dimethylamino derivative of norephedrine (15.6 g, 82%).

To a solution of *N,N*-dimethylamino norephedrine (15.2 g, 70.5 mmol) in CH_2Cl_2 (100 mL) was added thionyl chloride (20.6 mL, 282 mmol) in CH_2Cl_2 dropwise over 1 h. Addition of CCl_4 (200 mL) and cooling to 0 °C did not afford a solid, so the CH_2Cl_2 was distilled off and the remaining solution was chilled overnight to afford a pink solid, which was collected by filtration, rinsed with hexane (3) and dried. Recrystallization from acetone:MeOH (150 mL:5 mL) provided the (1*R*,2*R*) isomer of **17** (0.98 g) as light tan prisms. ^{1}H NMR ($CDCl_3$): δ 5.39 (1H, *J* = 7.6; CHCl). $[\alpha]_D^{25}$ = -110.9° (*c* = 1.0, MeOH).

[3R-[1(1R,2R*),3α,4α]]-1-[2-(Dimethylamino)-1-phenylpropyl]-1,3,4,5-tetrahydro-3-hydroxy-4-(4-methoxyphenyl)-6-trifluoromethyl-2H-1-benzazepin-2-one (18).*

To a suspension of NaH (93 mg, 1.93 mmol of a 50% oil dispersion) in dry DMF (4 mL) was added **16** (0.75 g, 1.61 mmol). The solution was stirred for 10 min, heated to 70 °C and a solution of **17** (0.87 g, 3.22 mmol) and KO*t*Bu (0.36 g, 3.22 mmol) in dry DMF (2 mL) was added. The reaction was stirred at 70 °C for 70 min, additional NaH (45 mg) and **17** (0.22 g) were added, and stirring continued for 90 min. The reaction was quenched with aqueous K_2CO_3, DMF was removed under vacuum with gentle warming, the residue partitioned between ether and aqueous K_2CO_3, washed with brine, dried ($MgSO_4$), and evaporated to afford a light yellow oil (1.51 g). Chromatography (SiO_2; EtOAc:hexane 2:3) provided the TBDMS ether of **18** as a colorless foamy solid (0.58 g).

The TBDMS ether of **18** (0.58 g) was dissolved in dry THF (25 mL) and tetrabutylammonium fluoride trihydrate (0.68 g, 1.56 mmol) was added in one portion. The solution was stirred for 20 min at r.t. and partitioned between ether and water. The aqueous layer was washed with ether and the combined organic layers were washed with brine, dried ($MgSO_4$), and evaporated to afford a gum (0.51 g). Chromatography on preparative TLC (SiO_2; 5% MeOH:CH_2Cl_2) and extraction (10% MeOH:0.5% Et_3N:CH_2Cl_2) provided the free base as a colorless foamy solid. The free base was dissolved in ether and treated with ethereal HCl. The resulting colorless precipitate was collected by filtration, rinsed with ether, and dried to afford **18** (205 mg) as a powdery solid. m.p. >220 °C. $[\alpha]_D^{25}$ = +180.0° (*c* = 1.0, MeOH). (M + H)$^+$ = 513. IR (KBr): 1669 cm^{-1}. Anal. ($C_{29}H_{31}F_3N_2O_3$·HCl) C, H, N, Cl, F. ^{1}H NMR ($CDCl_3$): δ 1.17 (d, 3H, *J* = 6.4), 1.83 (t, 1H, *J* = 13.5), 2.68 (dd, 1H, *J* = 5.3, 14.1), 3.06 (br d, 6H), 3.44 (m, 1H), 3.77 (s, 3H), 4.35 (d, 1H, *J* = 8.2), 4.47 (dd, 1H), 5.73 (br m, 1H), 6.81 (d, 2H, *J* = 8.8), 7.04 (d, 2H, *J* = 8.2), 7.35–7.68 (m, 8H), 10.83 (br s, 1H). ^{13}C NMR ($CDCl_3$): δ 12.3, 31.2, 37.5, 44.8, 50.9, 55.3, 62.7, 70.5, 71.8, 113.6, 127.9, 128.4, 129.0, 129.5, 129.7, 129.9, 130.9, 135.3, 135.6, 142.5, 158.7, 177.3.

[3R-[1(1S,2R*),3α,4α]]-1-[2-(Dimethylamino)-1-phenylpropyl]-1,3,4,5-tetrahydro-3-hydroxy-4-(4-methoxyphenyl)-6-trifluoromethyl-2H-1-benzazepin-2-one, isomer B (19)*

To a suspension of NaH (1.08 g, 22.6 mmol of a 50% oil dispersion) in dry DMF (10 mL) was added **16** (3.5 g, 7.52 mmol). The solution was stirred for 30 min, and a mixture of (1*S*,2*R*) and (1*R*,2*R*) **17** (mother liquors from the recrystallization of the 1*R*,2*R* compound; 3.05 g, 13 mmol)[28] was added as a solid, and the solution heated to 65 °C for 1 h. The solution was quenched with aqueous $NaHCO_3$, DMF was removed under vacuum with gentle warming, the residue partitioned between ether and aqueous K_2CO_3, washed with brine, dried ($MgSO_4$) and evaporated to provide a thick brown oil (6.18 g). Chromatography (SiO_2; ether:hexane 3:1, followed by EtOAc:hexane 3:1) afforded the crude TBDMS ether (1.18 g), which was purified further by chromatography (SiO_2; EtOAc:hexane 1:1) to provide the TBDMS ether as a yellow foamy solid (0.84 g, 18%).

The TBDMS ether was treated with tetrabutylammonium fluoride as described in the preparation of **18** to provide the hydrochloride salt. The hydrochloride salt was recrystallized from MeOH:*i*PE to afford **19** as a colorless powder (0.42 g, 0.76 mmol, 54%). m.p. 191–192 °C. $[\alpha]_D^{25}$ = +242.6° (c = 1.0, MeOH). (M + H)$^+$ = 513. IR (KBr): 1668 cm^{-1}. Anal. ($C_{29}H_{31}F_3N_2O_3$·HCl) C, H, N, Cl, F. ^{1}H NMR ($CDCl_3$): δ 1.96 (d, 3H, *J* = 6.4), 2.19 (dd, 1H, *J* = 13.5, 14.1), 2.42 (s, 3H), 2.60 (d, 1H, *J* = 10.0), 2.75 (dd, 1H, *J* = 5.3, 14.7), 2.97 (s, 3H), 3.52 (m, 1H), 3.83 (s, 3H), 4.21 (dd, 1H, *J* = 8.2, 10.0), 5.02 (m, 1H), 6.56 (d, 1H, *J* = 10.0), 6.93 (d, 2H, *J* = 8.8), 7.11 (d, 2H, *J* = 8.8), 7.63 (br s, 5H), 7.57–7.70 (m, 3H), 12.21 (br s, 1H). ^{13}C NMR ($CDCl_3$): δ 14.8, 31.1, 36.6, 44.2, 51.7, 55.3, 58.4, 61.9, 69.2, 114.0, 126.0, 128.1, 129.2, 129.4, 129.8, 130.0, 134.1, 135.2, 138.3, 159.3, 174.0.

Supplementary Material Available

Tables of unit cell data, atomic coordinates, and thermal parameters for compounds of Table 7 (28 pages).

This information may be obtained from the asterisked author.

Acknowledgement

Microanalyses, IR spectra, and mass spectra were kindly provided by the Bristol-Myers Squibb Department of Analytical Research and Development.

References

1. Floyd, D. M.; Moquin, R. V.; Atwal, K. S.; Ahmed, S. Z.; Spergel, S. H.; Gougoutas, J. Z.; Malley, M. F. Synthesis of benzazepinone and 3-methylbenzothiazepinone analogues of diltiazem. *J Org. Chem.* **1990**, *55*, 5572–5579.

2. Floyd, D. M.; Kimball, S. D.; Krapcho, J.; Das, J.; Turk, C. F.; Moquin, R. V.; Lago, M. W.; Duff, K. J.; Lee, V. G.; White, R. E.; Ridgewell, R. E.; Moreland, S.; Brittain, R. J.; Normandin, D. E.; Hedberg, S. A.; Cucinotta, G. G. Benzazepinone calcium channel blockers. 2. Structure–activity and drug metabolism studies leading to potent antihypertensive agents. Comparison with benzothiazepinones. *J. Med. Chem.* **1992**, *35*, 756–772.

3. Das, J.; Floyd, D. M.; Kimball, S. D.; Duff, K. J.; Vu, T. C.; Moquin, R. V.; Gougoutas, J. Z.; Malley, M. F.; Moreland, S.; Brittain, R. J.; Hedberg, S. A.; Cucinotta, G. G. Benzazepinone calcium channel blockers. 3. Synthesis and structure–activity studies of 3-alkyl benzazepinones. *J. Med. Chem.* **1992**, *35*, 773–780.

4. Kimball, S. D.; Floyd, D. M.; Das, J.; Hunt, J. T.; Krapcho, J.; Rovnyak, G.; Duff, K. J.; Lee, V. G.; Moquin, R. V.; Turk, C. F.; Hedberg, S. A.; Moreland, S.; Brittain, R. J.; McMullen, D. M.; Normandin, D. E.; Cucinotta, G. G. Benzazepinone calcium channel blockers. 4. Structure-activity overview and intracellular binding site. *J. Med. Chem.* **1992**, *35*, 781–793.

5. Das, J.; Floyd, D. M.; Kimball, S. D.; Duff, K. J.; Lago, M. W.; Krapcho, J.; White, R. E.; Ridgewell, R. E.; Obermeier, M. T.; Moreland, S.; McMullen, D.; Normandin, D.; Hedberg, S. A.; Schaeffer, T. R. Benzazepinone calcium channel blockers. 5. Effects on antihypertensive activity associated with N1 and aromatic substituents. *J. Med. Chem.* **1992**, *35*, 2610–2617.

6. Kimball, S. D.; Floyd, D. M.; Barrish, J. C.; Das, J.; Hunt, J. T.; Krapcho, J.; Rovnyak, G.; Duff, K. J.; Lago, M.; Lee, V. G.; Moquin, R. V.; Spergel, S.; Gougoutas, J. Z.; Malley, M.; Pudzianowski, A.; Flaim, S. F.; Moreland, S.; Hedberg, A.; White, R. E. Structure activity studies and receptor binding model of 1-benzazepin-2-one calcium antagonists. In *Trends in Medicinal Chemistry* '90, pp. 271–276, Sarel, S., Mechoulam, R., Agranat, I. Eds.; Blackwell Scientific Publications; Oxford, **1992**.

7. Kimball, S. D. *The Design of New Calcium Antagonists*, AAAS Publications (1993) *in press*.

8. Kojie-Prodic, B.; Ruzic-Toros, Z.; Sunjie, V.; Decorte, E.; Moimas, F. Absolute conformation and configuration of (2*S*,3*S*)-3-acetoxy-5-(dimethylaminoethyl) -2-(4-methoxyphenyl)-2,3-dihydro-1,5-benzothiazepin-4(5*H*)-one chloride (dilthiazem hydrochloride). *Helv. Chim. Acta* **1984**, *67*, 916–926.

9. Glaser, R.; Sklarz, B. Stereochemistry and conformation in solution of diltiazem hydrochloride, a 1,5-benzothiazepine coronary vasodilator. *J. Chem. Soc. Perkin Trans. II* **1989**, 1031–1036.

10. Compound **7** was prepared from cyclohexene oxide as described in the literature: Paris, O. E.; Fanta, P. E. *J. Am. Chem. Soc.* **1952**, *74*, 3007; Taguchi, T.; Eto, M. *J. Am. Chem. Soc.* **1958**, *80*, 4075–4079.

11. The 3*S*-*trans* tosylate **10** was prepared from hydroxyproline by decarboxylation (*Chem. Lett.* **1986**, 895), *N*-benzylation (BnCl, PTC), inversion of the alcohol center (PhCOOH, DEAD, Ph_3P; then NaOH), and tosylation (TsCl, pyridine). The 3*R* analog was prepared by the same sequence without inversion of stereochemistry.

12. β-Chloro-phenethylamine **13** was prepared as described in the literature; Meyers, B. N.; Helfrich, J. S.; Nichols, D. E.; McLaughlin, J. L. *J. Nat. Prod.* **1983**, *46*, 688–693.

13. An aziridinium intermediate is consistent with all of the chemistry of benzazepinones that we have carried out. This mechanism is described for a related β-chloro-phenethylamine in Ref. 12.

14. See, for example: (a) *Reviews of Physiology, Biochemistry, and Pharmacology* **1990**, *114*. Springer Verlag; Berlin. (b) Triggle, D. J. *In Cardiovascular Pharmacology*, pp. 107–160, Antonaccio, Ed.; Raven Press: New York, 1990.

15. Glossmann, H.; Ferry, D.R.; Goll, A.; Striessnig, J.; Schober, M. Calcium channels: basic properties as revealed by radioligand binding studies. *J. Cardiovascular Pharmacology.* **1985**, *7 (Suppl. 6)*, S20–S30.

16. Triggle, D. J.; Langs, D. A.; Janis, R. A. In *Medicinal Research Reviews*, deStevens, Ed.; J. Wiley; New York, 1988.

17. Catterall, W.A.; Striessnig, J. Receptor sites for Ca^{2+} channel antagonists. *TiPS* **1992**, *13*, 256–262.

18. (a) Garcia, M. L.; King, V. F.; Siegl, P. K. S.; Rueben, J. P.; Kaczorowski, G. J. Binding of Ca^{2+} entry blockers to cardiac sarcolemmal membrane vesicles. *J. Biol. Chem.* **1986**, *261*, 8146–8157 (b) Striessnig, J. personal communication of work currently in press (AAAS publications, 1993).

19. (a) Ruth, P.; Flockerzi, V.; von Nettelbladt, E.; Oeken, J.; Hofmann, F. Characterization of the binding sites for nimodipine and (−)-desmethoxyverapamil in bovine cardiac sarcolemma. *Eur. J. Biochem.* **1985**, *150*, 313–322. (b) Sieber, M.; Nastainczyk, W.; Rohrkasten, A.; Hofmann, F. Reconstitution of the purified receptor for calcium channel blockers. *Biomed. Biochim. Acta* **1987**, *46*, S357–S362.

20. Striessnig, J.; Goll, A.; Moosburger, K.; Glossmann, H. Purified calcium channels have three allosterically coupled drug receptors. *FEBS Lett.* **1986**, *197*, 204–210.

21. Reynolds, I. J.; Snowman, A. M.; Snyder, S. H. (−)-[^{3}H] Desmethoxyverapamil labels multiple calcium channel modulator receptors in brain and skeletal muscle membranes: differentiation by temperature and dihydropyridines. *J. Pharm. Exp. Ther.* **1986**, *237*, 731–738.

22. (a) Mannhold, R.; Kaufmann. R. The cellular site of action of heart-active drugs. *Arch. Pharm. (Weinheim)* **1986**, *319*, 1028–1036. (b) Hescheler, J.; Pelzer, D.; Trube, G.; Trautwein, W. Does the organic calcium channel blocker D600 act from inside or outside on the cardiac cell membrane? *Pfluegers Arch. Physiol.* **1982**, *393*, 287–291. (c) White, E. J.; Bradford, H. F. Participation of intracellular sites in the action of Ca^{+2} channel blockers. *Eur. J. Pharmacol.* **1986**, *130*, 243.

23. Allen, F. H.; Kennard, O.; Taylor, R. Systematic analysis of structural data as a research technique in organic chemistry. *Acc. Chem. Res.* **1983**, *16*, 146 153.

24. Gougoutas, J. Z. and Hermsmeier, M. A. Unpublished results.

25. Carpy, A.; Leger, J.-M.; Melchiorre, C. Structure of α-isopropyl-α-[(*N*-methyl-*N*-homoveratryl)-γ-aminopropyl]-3, 4-dimethoxyphenylacetonitrile hydrochloride, * Verapamil, $C_{27}H_{38}N_2O_4$·HCl *Acta Cryst. C* **1985**, *41*, 624.

26. Main, P.; Lessinger, L.; Woolfson, M. M.; Germain, G.; Declercq, J. P. MULTAN 78; University of York (U.K.) and Louvain (Belgium), 1978.

27. SDP, Structure Determination Package, A Frenz & Associates, College Station, TX 77840. Scattering factors, including f and f'', in the SDP software were taken from the *International Tables for Crystallography*; Vol. 4, Tables 2.2A and 2.3.1, Kynoch Press: Birmingham, U.K., 1974.

28. A sample of the mother liquors was purified by preparative TLC to provide pure 1*R*,2*R* compound **17** (J = 7.63) as described in the preparation, and the other component, which was determined to be pure 1*S*,2*R* diastereomer (J = 0 Hz). For convenience, the mixture of diastereomers **17** was used in the preparation of **19**.